Indirect Interaction between Adatoms on a Tight-Binding Solid*

T. L. Einstein and J. R. Schrieffer
Department of Physics, University of Pennsylvania, Philadelphia, Pennsylvania 19104
(Received 24 July 1972)

The indirect interaction between adatom pairs on the (100) surface of a simple-cubic tight-binding solid is investigated within a molecular-orbital approach. A general scheme for calculating the surface-density-of-states change and the interaction energy of one and two single-level adatoms is presented, and contact (and a correction) is made with Grimley's formulation. The method permits binding above surface atoms, at bridge sites, or at centered positions, and yields interaction energy as a function of band filling, adatom energy level, and a general hopping potential V between an adatom and the nearest surface atom(s). Calculations have been carried out for V/W_b in the range 1/12–1/2, the upper limit giving split-off states ($W_b \equiv$ bandwidth). The single-atom interaction shows little dependence on binding type, in all three cases being most attractive when the Fermi energy equals the noninteracting adatom level, with a strongly V-dependent strength. For the pair interaction, one finds a strength at nearest-neighbor separation of about an order of magnitude smaller than the absorption energy of a single adatom. This interaction has an exponentiallike dropoff and sign alternations as one moves along the ⟨10⟩ direction. Under reasonable conditions, the nearest-neighbor interaction is often repulsive while the next nearest, third nearest, or fourth nearest is attractive, suggesting the patterns $c(2\times 2)$, (2×2), and $c(4\times 2)$, respectively, which are frequently observed in the adsorption of simple gases on the (100) surfaces of transition metals. On the basis of two-dimensional Ising-model calculations including second-neighbor interactions, one can estimate the strength of V from the observed disordering temperature of the adatom lattice; the result is similar to that obtained from estimates based on the heat of adsorption.

I. INTRODUCTION

An intriguing aspect of the chemisorption of simple gases onto transition metals is the variety of surface structures observed. Below a critical temperature, the pattern within surface adlayer islands is highly dependent on the substrate, but not always are these arrays identical in structure to the surface layer of the adsorbate. The nearest site occupied (relative to some occupied site) is often the second, third, or even fourth nearest neighbor rather than the (first) nearest neighbor.[1] Over a decade ago, Koutecký[2] deduced that these adatoms interact (share electrons) via the substrate-metal electron band and therefore exhibit oscillatory behavior reminiscent Ruderman–Kittel–Kasuya–Yosida (RKKY) interactions.[3] In the last several years, Grimley[4–6] and Newns[7] have formalized this "indirect interaction" on the basis of the analogy to the Anderson model for dilute magnetic impurities.[8] However, the interaction energy has only been evaluated in the asymptotic regime and/or in the simple (and often invalid) approximation that a virtual level could describe the interaction.

This paper presents a first attempt at the theoretical evaluation of the two-adatom indirect interaction at nearby binding sites. As such, we have allowed ourselves a number of simplifying assumptions. We deal with the (100) surface of a simple cubic semi-infinite lattice, using the formalism and program of Kalkstein and Soven[9] to obtain surface Green's functions. Since we are interested in covalent binding, we work with transition-metal substrates, as these provide the strongest bond. A tight-binding model replicates the d band, and the sp band is neglected, as in Grimley[4] and Newns.[7] Thus the possibility of hybridization as an explanation for H on a W (100) surface, suggested by Tamm and Schmidt,[10] is excluded from the beginning. The adatoms are assumed to have a single energy level, a reasonable approximation for a simple gas atom or an atom with a partially filled d shell. Correlation effects are not considered explicitly, but can be roughly accommodated by self-consistently adjusting the parameters of the problem, such as the adatom level. This approximation is reasonable in systems where there is only a weak tendency toward localized-moment formation on the adsorbate, i.e., $U/\pi\Gamma < 1$, where U is the Coulomb repulsion and Γ is a measure of the half-width of the adsorbate density of states, corresponding to the conventional half-width in the case of a Lorentzian level.

In Sec. II we describe our general calculational method for dealing with the single-adatom and pair-interaction problems. The method extends easily and naturally to the three-or-more-body problem but this generality is not required to explain surface patterns. Since the n-body interaction energy falls off by an order of magnitude for each additional particle (at least for n small) we

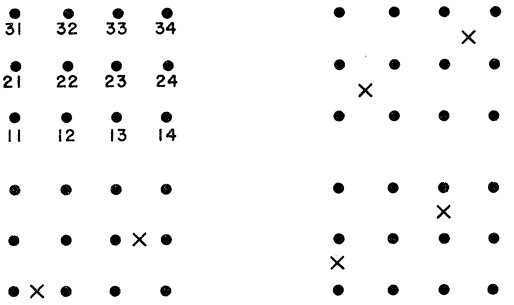

FIG. 1. Charts indicating the labeling convention for the binding of adatom pairs on the (100) surface of a simple cubic crystal, and the four possible types of binding. The first diagram shows atop (A) binding. One adatom is always taken to bind to site (11); the second can sit at any other side, and that site then labels the interaction. Thus, the pair-interaction energy and the Green's function corresponding to this chart are referred to as ΔW^A_{23} and G^A_{23}, respectively. The other charts describe the 23 interactions for centered (C), bridge(B), and bridge-perpendicular (BP) binding.

need only consider the one- and two-body terms. The calculations distinguish binding directly above the surface (called "atop" or A here, "and on-site" or "linear" sometimes elsewhere), at a centered site (symmetrically between four surface atoms; called C), or at a bridge site (symmetrically between two; called B). In the last case, we distinguish bridge B and bridge-perpendicular BP binding in the pair problem: In the former case, a line joining the two surface neighbors of an adatom tends to be parallel to a line joining the two adatoms (i.e., the angle between them is less than 45°); in the latter case, the lines are more nearly perpendicular (angle greater than 45°). If the two adatoms sit diagonally, the two cases become identical. Figure 1 illustrates the four binding symmetries, and also describes our labeling convention for surface sites: We label sites by the subscripts (ij) of a square lattice, so that (11) is the "origin" and i, j are generally positive integers—symmetries in the interaction energy, and ultimately the surface Green's functions, allow all discussions to be framed in terms of one quadrant of the plane. In dealing with the problem of adatom pairs, we will denote the location of one adatom by (11) [i.e., the lattice site (11) or the associated symmetry site, as illustrated in Fig. 1] and the other adatom at some other (ij). Since the pair interaction tends to be weaker than the variation in single-adatom adsorption energy with binding symmetry, we calculate here only the case that both adatoms select the same binding symmetry. It is straightforward to generalize the calculations to a more general situation. The pair interaction then determines the configuration within an island of adatoms: After the first adatom bonds, we visualize a second adatom approaching the surface nearby. Since any site (with the same binding symmetry as the first) will provide the same one-body energy lowering, it is the pair interaction which determines the most favorable position for this second adatom. Correspondingly, a third adatom will bind with the same site symmetry as the first two at a relative position that is most favorable in terms of the sum of its two-body interactions with them. We view this process as continuing as more adatoms join the domain. Thus, from a chart of the pair interaction it is generally easy to determine the structure of an island.

Section II discusses in detail the analytic properties of the solution. Contact is made with Grimley's work,[4,6] and many of his approximations and derivations (that parallel ours) are discussed.

The reader who is principally interested in calculational results should refer directly to Sec. III, where computations for the interaction energy for a single adsorbed atom and between two nearby adatoms are presented. General characteristics for a large range of input parameters are described, and experimental information (binding energy, surface-array critical temperature for disordering, probability of occurrence of particular adlayer patterns) is used to evaluate the adatom-surface hopping parameter and to check that the calculational results are reasonable. Section IV summarizes the investigation and discusses possible extensions.

II. MODEL

A. Green's Functions

In our model we consider a perturbed Hamiltonian of the form $\mathcal{H}=\mathcal{H}_0+V$. $\mathcal{H}_0$ is the Hamiltonian for a semi-infinite solid, with eigenstates $|k\rangle$ and eigenvalues ϵ_k plus the Hamiltonian for the isolated adatoms relevant to the problem, one or two here, with eigenvalue E_a. The potential V connects the adatom state $|a\rangle$ with a binding site $|i\rangle$, allowing hopping between them. In this paper we restrict ourselves for simplicity to the (100) face of a simple cubic crystal. $|ij\rangle$ denotes the Wannier function associated with site (ij). For binding directly above a surface atom, $|i\rangle=|11\rangle$; for binding at a bridge site,

$$|i\rangle=(|11\rangle+|12\rangle) \quad [\text{or } |i\rangle=(|11\rangle+|21\rangle)] \ ;$$

and for binding at a centered site,

$$|i\rangle=\tfrac{1}{2}(|11\rangle+|12\rangle+|21\rangle+|22\rangle) \ .$$

The semi-infinite metal $\mathcal{H}_0$ we use here is that of Kalkstein and Soven,[9] since we will use their Green's-function calculational technique in comput-

ing the interaction energy. Using linear-combination-of-atomic-orbitals (LCAO) or tight-binding formalism, the most realistic simple approximation for d-band metals, they start out with a perfect-crystal Hamiltonian $\mathcal{H}_0$ with only one-center and nearest-neighbor two-center real-space matrix elements. The one-center element, i.e., the atomic-orbital self-energy, implicitly defines their energy zero. We take their isotropic two-center element E_1 to be $-T$, where T is a positive number. In three dimensions, these choices lead to an energy band of width $W_b = 12T$, which is centered at the energy zero. Unless otherwise stated, we will measure energy in units of $2T$ (or equivalently $\frac{1}{6}W_b$), and will thus drop $2T$ when clarity does not require it. Kalkstein and Soven then add a potential to cancel interactions across the cleavage line (which divides the metal into semi-infinite halves), and a perturbation U to account for surface effects such as electron redistribution. Since we are not putting in Coulomb correlations, we neglect U. Invoking periodicity in the two directions parallel to the surface, one can show that the one-electron Green's function for an atom on the perfect surface is

$$G_{11}(E, \vec{k}_{\parallel}) = (1/2T^2)[+\omega + i(4T^2 - \omega^2)^{1/2}] \ , \qquad (2.1)$$

where for our simple surface

$$\omega = E + 2T(\cos k_x a_0 + \cos k_y a_0) \ , \qquad (2.2)$$

a_0 being the lattice parameter and the root is $+i\,\mathrm{sgn}\omega\,(\omega^2 - 4T^2)^{1/2}$ for $\omega^2 > 4T^2$. To obtain this "atop" surface Green's function, one must perform a sum over the surface Brillouin zone:

$$G^A_{11,ij} \equiv G^A_{ij}(E) = \sum_{|k_x|,\,|k_y| \le \pi/a} G_{11}(E, \vec{k}_{\parallel}) e^{i\vec{k}_{\parallel}\cdot(\vec{R}_{ij} - \vec{R}_{11})} \ . \qquad (2.3)$$

Since the first index of G will generally be 11, one can usually omit it, as indicated, with no loss of clarity. The following remarks concerning the Green's functions calculated by the Kalkstein–Soven program are helpful in the subsequent analysis.

(i) The atop diagonal Green's function can be rather well approximated by a triangular density of states (with E in units of $2T$)—although this simplification was not employed in the present calculations:

$$\mathrm{Im}G_{\Delta}(E) = \begin{cases} \frac{1}{3}\pi(1 - \frac{1}{3}|E|), & |E| < 3 \\ 0 \ , & |E| > 3 \end{cases} \qquad (2.4)$$

$$\mathrm{Re}G_{\Delta}(E) = \tfrac{1}{9}E \ln\left|\frac{(3+E)(3-E)}{E^2}\right| + \tfrac{1}{3}\ln\left|\frac{3+E}{3-E}\right| \ .$$

The sharp corners of the triangle obviously are smoothed in the actual result. This gives a better fit than the semi-elliptical density of states of the one-dimensional chain[7]:

$$\mathrm{Im}G_{\Delta}(E) = \begin{cases} \frac{2}{9}(9 - E^2)^{1/2}, & |E| < 3 \\ 0, & |E| > 3 \end{cases} \qquad (2.5)$$

$$\mathrm{Re}G_{\Delta}(E) = \begin{cases} \frac{2}{9}E, & |E| < 3 \\ \frac{2}{9}[E \mp (E^2 - 9)^{1/2}], & |E| > 3 \text{ and } E \gtrless 0. \end{cases}$$

(ii) As suggested in (i), the imaginary part of $G^A_{11}(E)$ is symmetric about $E = 0$, the center of the band, while $\mathrm{Re}G^A(E)$ is antisymmetric. This result arises as follows. $G_{11}(E, \vec{k}_{\parallel})$ is symmetric in $\vec{k}_{\parallel}$, i.e., k_x and k_y: $G_{11}(E, k_{\parallel}) = G_{11}(\omega(E, k_{\parallel}))$, where $\omega = E + 2T(\cos k_x a_0 + \cos k_y a_0)$, and $\cos k a_0$ is symmetric in k. Hence the sum over $-\pi/a < k_x$, $k_y < \pi/a$ can be reduced to four times the sum over a quadrant, say, $0 < k_x$, $k_y < \pi/a$. If we let $k_x \to \pi/a - k_x$, $k_y \to \pi/a - k_y$, and $E \to -E$, then the region of summation remains the same, but ω changes sign. From the explicit form of $G_{11}(E, \vec{k}_{\parallel})$ given in (2.1), it is obvious that $\mathrm{Re}G_{11}(-\omega) = -\mathrm{Re}G_{11}(\omega)$ and $\mathrm{Im}G_{11}(-\omega) = \mathrm{Im}G_{11}(\omega)$. Since this is true for all $k_{\parallel}$, and hence for all $k_{\parallel}$ in the quadrant, the symmetries of $\mathrm{Re}G^A_{11}(E)$ and $\mathrm{Im}G^A_{11}(E)$ follow. The fact that the real and imaginary parts of G have opposite symmetry can be viewed as a result of the fact that they satisfy a Kramers–Kronig relation.

(iii) The symmetry of $G^A_{11,ij}(E)$ alternates with each lattice spacing of separation, i.e.,

$$\mathrm{Im}G^A_{ij}(-E) = (-1)^{m+n}\mathrm{Im}G^A_{ij}(E), \qquad \mathrm{Re}G^A_{ij}(-E) = -(-1)^{m+n}\mathrm{Re}G^A_{ij}(E) \ , \qquad (2.6)$$

where $m = i - 1$ and $n = j - 1$. By using the symmetry in $k_{\parallel}$ which permits the reduction of the $k_{\parallel}$ sum to a quadrant, we see that the contribution of $e^{i\vec{k}_{\parallel}\cdot(\vec{R}_{ij} - \vec{R}_{11})}$ is just $\cos mk_x a_0 \cos nk_y a_0$. In performing the ω inversion of (ii), i.e., $k_x \to \pi/a - k_x$, etc., we use the fact that

$$\cos mk_x a_0 = (-1)^m \cos m(\pi - k_x a)$$

and similarly for k_y, and the above symmetry is obtained.

(iv) Since, as we saw in (iii), the distance factor enters only through the factor $\cos mk_x a_0 \cos nk_y a_0$, we can write down various mirror equalities [where the 2's are required by our choice of (11) rather than (00) as the origin]:

$$G^A_{2-i,j}(E) = G^A_{ij}(E) = G^A_{i,2-j}(E) \qquad (2.7)$$

to account for Green's functions outside the quadrant i, $j \ge 1$. Moreover, by the symmetry in k_x and k_y in the summation, we find $G^A_{ij}(E) = G^A_{ji}(E)$. With the aid of these three equalities, we can write any Green's function $G^A_{kl,k'l'}(E)$ as $G^A_{ij}(E)$, where j is the larger of $|k - k'| + 1$ and $|l' - l| + 1$, and i is the smaller; that is, we can reduce all formulas in G^A into expressions of G^A's in the octant between $\langle 10 \rangle$ and $\langle 11 \rangle$, inclusive.

(v) It is easy to check that $\mathrm{Im}G^A_{ij}(E)$ vanishes outside the band, i.e., for $|E| \geq 3$. Then ω^2 is always ≥ 1 (i.e., $4T^2$), so that there is no imaginary part in $G_{11}(E, \vec{k}_\parallel)$. For E just above the bottom of the band, $\omega^2 < 1$ only for k_x and k_y nearly zero, so that $\cos k_x a_0 + \cos k_y a_0 \approx 2$. For such E, the leading factors $\cos mk_x a_0 \cos nk_y a_0$ will be near unity, or at least positive. Hence we have the general result that for any ij, $\mathrm{Im}G^A_{ij}(E)$ increases from zero as one initially increases energy from the bottom of the band: the extremum nearest the bottom is positive. By similar but more tortuous reasoning, or more simply by looking at the Kramers–Kronig relation

$$\mathrm{Re}G^A_{ij}(E) = -\frac{1}{\pi}\mathcal{P}\int_{-\infty}^{\infty}\frac{\mathrm{Im}G^A_{ij}(E')}{E'-E}dE' \ ,$$

one verifies that $\mathrm{Re}G^A_{ij}(E)$ is negative at the bottom of the band, for any ij. A more detailed look shows that $\mathrm{Im}G(E)$ is initially proportional to the $\frac{3}{2}$ power of the magnitude of energy difference from the upper- or lower-band edge.

(vi) The number of extrema in the parts of G^A_{ij} increases rapidly with i and j. For $i, j \leq 3$, there are $i+j-1$ $(m+n+1)$ extrema in $\mathrm{Im}G^A_{ij}(E)$, or equivalently, there are $m+n$ internal zeros, or $i+j$ zeros including endpoints. If i or $j \geq 4$, there are more than $m+n+1$ extrema, although no simple empirical formula seems to fit the computational result. For use in Sec. III, we point out in particular that $(ij) = (14)$, (15), and (16) have 4, 9, and 10 extrema in $\mathrm{Im}G^A_{ij}(E)$, respectively. From (iii), we find that if one of the indices is raised by one, the number of extrema must increase by an odd number. With the Kramers–Kronig relation one can demonstrate the observed result that $\mathrm{Re}G^A_{ij}(E)$ has one extremum more than $\mathrm{Im}G^A_{ij}(E)$.

To determine the Green's function for other binding positions, we note that

$$G^A_{ij}(E) = \left\langle ij \left| \frac{1}{E - \mathcal{H} - i\delta} \right| 11 \right\rangle \qquad (2.8)$$

formally. To express bridge binding of the same separation, $a_0[(i-1)^2 + (j-1)^2]^{1/2}$, with the adatom's surface neighbors both in the same row (for $i \leq j$), we substitute

$$G^B_{ij}(E) = G^A_{ij}(E) + \tfrac{1}{2}\left[G^A_{i,j-1}(E) + G^A_{i,j+1}(E)\right] \ . \qquad (2.9)$$

The choice of the symmetric combination of perturbed atomic orbitals indicates the selection of the bonding state, i.e., the combination lowering the metallic energy distribution $\Delta\rho^X_{ij}(E) = (1/\pi)\mathrm{Im}G^X_{ij}(E)$. Section III elaborates on this manifestation of the importance of the symmetry of the orbitals, describing the skewing of $\Delta\rho^X_{ij}(E)$ and its effect on the binding energy of adatoms. Alternatively, to have the antidomain, with the bridge neighbors in the same column, we would substitute

$$|11\rangle_{BP} = \tfrac{1}{2}(|11\rangle + |21\rangle)$$

and

$${}_{BP}\langle ij| = \tfrac{1}{2}(\langle ij| + \langle i+1, j|) \ ,$$

respectively, to get

$$G^{BP}_{ij}(E) = G^A_{ij}(E) + \tfrac{1}{2}\left[G^A_{i-1,j}(E) + G^A_{i+1,j}(E)\right] \ . \qquad (2.10)$$

The assumption $1 \leq i \leq j$ is convenient, and possible, as elaborated in remark (iv). Moreover, should an index not be positive in a general formula, remark (iv) indicates how to reduce the errant G^A to the selected octant. Thus, for example, $G^B_{11} = G^A_{11} + G^A_{12}$. Note also that $G^{BP}_{ii} = G^B_{ii}$. Finally, for centered binding, one makes substitutions of the form

$$|ij\rangle_C = \tfrac{1}{4}(|ij\rangle + |i+1, j\rangle + |i, j+1\rangle + |i+1, j+1\rangle)$$

for $|ij\rangle$ to find, for example, that $G^C_{11} = G^A_{11} + 2G^A_{12} + G^A_{22}$, using the two mirror symmetries of (iv). Figure 1 illustrates the different types of binding.

We present two additional remarks concerning the surface Green's functions with any of the four binding position symmetries.

(vii) $\mathrm{Im}G^B_{11}(E)$ and $\mathrm{Im}G^C_{11}(E)$ are both positive throughout the band. Recall

$$\mathrm{Im}G^B_{11}(E) = \mathrm{Im}G^A_{11}(E) + \mathrm{Im}G^A_{12}(E) = \sum_{k_x, k_y}(1 + \cos k_x a_0)\,\mathrm{Im}G(E, \vec{k}_\parallel) \ ,$$

where $\mathrm{Im}G(E, \vec{k}_\parallel) \geq 0$. But $1 + \cos k_x a_0 \geq 0$. Similarly, for $\mathrm{Im}G^C_{11}(E)$, the factor is

$$(1 + \cos k_x a_0 + \cos k_y a_0 + \cos k_x a_0 \cos k_y a_0) = (1 + \cos k_x a_0)(1 + \cos k_y a_0) \geq 0 \ .$$

By the symmetry in k_x and k_y, one might write

$$(1 + 2\cos k_x a_0 + \cos k_x a_0 \cos k_y a_0)$$

in actually performing the sum. Figure 3, which reproduces the calculated $\mathrm{Im}G^X_{11}$, confirms the claim of this remark.

(viii) $\mathrm{Im}G^A_{11}(E) \geq |\mathrm{Im}G^A_{ij}(E)|$, i.e., $\mathrm{Im}G^A_{11}(E) \mp \mathrm{Im}G^A_{ij}(E) \geq 0$. This difference (sum) is just the sum over the positive $G_{11}(E, \vec{k}_\parallel)$ times the factor

$$1 \mp \cos(mk_x a_0)\cos(nk_y a_0) \geq 0.$$

More generally, we can apply the Schwarz inequality since $\mathrm{Im}G^X_{ij}$ is a Hermitian inner product on a Hilbert space:

$$({}_X\langle ij|, |kl\rangle_X) \equiv {}_X\left\langle ij \left| \mathrm{Im}\frac{1}{E - \mathcal{H} - i\delta} \right| kl \right\rangle_X \ .$$

Thus

$$|\mathrm{Im}G^X_{ij}(E)| = |({}_X\langle ij|, |11\rangle_X)| \leq [({}_X\langle ij|, |ij\rangle_X)({}_X\langle 11|, |11\rangle_X)]^{1/2}$$

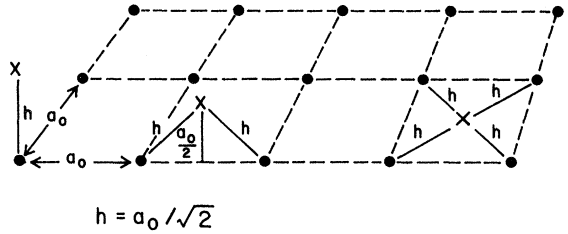

FIG. 2. Diagram illustrating a possible system in which V is the same for atop (A), bridge (B), and centered (C) binding: for approximately spherically symmetric orbitals this statement about the potential is true if the adatom is the same distance h from its nearest substrate neighbor(s) regardless of binding type. The minimum value for h is $a_0/\sqrt{2}$, for which a "centered" adatom lies in the surface plane. Although convenient, the assumption of the same V for all binding types is not at all necessary in our analysis.

$$= \left|\mathrm{Im}G^X_{11}(E)\right| = \mathrm{Im}G^X_{11}(E) \quad , \qquad (2.11)$$

where the last step follows from (vii), and the preceding step from surface translational lattice symmetry.

The potential V represents the entire interaction of an atom with the bulk; we assume no overlap with nearby adatoms. V is nondiagonal. It has the form V_{a1}, or $V_{1a} = V^\dagger_{a1}$, where small italic letters denote an adatom's noninteracting level and numbers signify a surface atom. We define $V = |V_{a1}|$. For atop binding, an adatom electron can hop only onto the bulk atom just below it. For bridge (center) binding, it can hop to any of the two (four) nearest metal atoms. This potential parameter can be scaled separately for each of the three binding positions to fit single-adatom binding energies. For the sake of comparison, it is convenient to assume that regardless of binding type, the hopping potential has the same strength: $V_{in} = V_{a1}$ if adatom i and surface atom n are nearest neighbors, and 0 otherwise. This assumption would certainly be justified in the case of spherical orbitals and similar adatom–surface-atom distances for the three types of binding. If we take the adatom to be in the surface plane for centered binding, then this distance h is $a_0/\sqrt{2}$, where a_0 is the lattice constant. An atop adatom would be assumed to be this far above the surface, while for bridge binding it is $\frac{1}{2}a_0$ above the surface (45° angle) (cf. Fig. 2). This scenario is not at all unreasonable as a first approximation, and we shall see that for single-atom binding, one gets very similar binding energies for the three types at fixed V.

B. Interaction Energy

1. Basic Formation

A general method to calculate the change in the density of states of a perturbed Hamiltonian $\mathcal{H} = \mathcal{H}_0 + \hat{V}$ ($\mathcal{H}$ and $\mathcal{H}_0$ have eigenvalues E_j and ϵ_j, respectively) can be derived as follows. We observe that

$$\mathrm{Det}\left(\frac{1}{E - \mathcal{H}_0 - i\delta}\right)(E - \mathcal{H} - i\delta) = \prod_j \frac{E - E_j - i\delta}{E - \epsilon_j - i\delta} \quad . \qquad (2.12)$$

Thus we can write

$$\frac{1}{\pi}\,\mathrm{Im}\,\frac{\partial}{\partial E}\ln\det\left(\frac{1}{E - \mathcal{H}_0 - i\delta}\right)(E - \mathcal{H} - i\delta)$$

$$= \frac{1}{\pi}\,\mathrm{Im}\sum_j\left(\frac{1}{E - E_j - i\delta} - \frac{1}{E - \epsilon_j - i\delta}\right)$$

$$= \sum_j \left[\delta(E - E_j) - \delta(E - \epsilon_j)\right] = \Delta\rho \quad . \qquad (2.13)$$

If we define $G^0 = (E - \mathcal{H}_0 - i\delta)^{-1}$, then

$$\det\left(\frac{1}{E - \mathcal{H}_0 - i\delta}\right)(E - \mathcal{H} - i\delta) = \det(1 - G^0\hat{V})$$

so that

$$\Delta\rho = \frac{1}{\pi}\,\mathrm{Im}\,\frac{\partial}{\partial E}\ln\det(1 - G^0\hat{V}) \quad . \qquad (2.14)$$

We select the representation with the eigenstates of $\mathcal{H}_0$ as basis vectors, so that G^0 is diagonal, and the mn matrix element has the form $\delta_{m,n} - G^0_{m,m}\hat{V}_{mn}$. If $\hat{V}$ has matrix elements only between a set of states 1, . . . , n, then outside the $n \times n$ submatrix in the upper left-hand corner, one will have only 1's along the diagonal and 0 off it. Thus, the determinant of the matrix is that of the submatrix.

As Grimley[4] discusses, conservation of electrons implies

$$\int_{-\infty}^{E_F} \rho\, dE - \int_{-\infty}^{E_F^0} \rho_0\, dE = 0$$

or

$$\int_{-\infty}^{E_F} \Delta\rho\, dE = -\,\Delta E_F\,\rho_0(E_F) \quad , \qquad (2.15)$$

where $\Delta\rho = \rho - \rho_0$. Hence

$$\Delta W = 2\left(\int_{-\infty}^{E_F} E\rho\, dE - \int_{-\infty}^{E_F^0} E\rho_0 dE\right)$$

$$= 2\left\{\int_{-\infty}^{E_F}\left[E\,\Delta\rho + E_F\,\Delta E_F\,\rho_0(E_F)\right]dE\right\}$$

$$= 2\int_{-\infty}^{E_F} (E - E_F)\Delta\rho\, dE \quad . \qquad (2.16)$$

The factor of 2 accounts for electron-spin degeneracy. This proof works for infinitesimal ΔE_F, which is the case for a very large system. Henceforth, we can let $E_F = E_F^0$. Inserting our expression (2.14) for $\Delta\rho$ and integrating by parts, we find

$$\Delta W = -\,(2/\pi)\int_{-\infty}^{E_F} \mathrm{Im}\ln\det(1 - G^0V)dE. \qquad (2.17)$$

Let us investigate this expression for adsorption of one and two atoms. For the single atom, $\hat{V}$ connects only the states a and 1 (where 1 may be

a symmetric combination ofstates). Thus

$$\det\begin{pmatrix} 1 & -G_{aa}V_{a1} \\ -G_{11}^X V_{1a} & 1 \end{pmatrix} = 1 - G_{aa}G_{11}^X V^2 \qquad (2.18)$$

and

$$\Delta W_{\text{single}}^X = -\frac{2}{\pi}\int_{-\infty}^{E_F} \operatorname{Im}\ln\left(1 - \frac{V^2 G_{11}^X(E)}{E - E_a - i\delta}\right) dE \ . \qquad (2.19)$$

The form of the determinant indicates that we are calculating the interaction for an electron hopping from the adatom to the nearest solid atom, interacting with the metallic d band, and then hopping back to the adatom orbital. $G_{11}^X(E)$ is shorthand for $G_{11,11}^X(E)$, as discussed above, where $X = A$, B, BP, and C. Recalling that Im ln is just the arctangent, we note that for small V, $\Delta W \propto V^2$, the perturbation-theory prediction. For V very large (relative to the band width W_b), the integrand approaches $\tan^{-1}(V^2 \operatorname{Im} G_{11}^X / V^2 \operatorname{Re} G_{11}^X)$. Hence the integral over the band approaches a constant (with respect to V). In addition, there is a pole term arising from a split-off state. As discussed later in this section, the split-off contribution, and hence ΔW, is linear in V for large potential. In this regime, the adatom and nearby surface atoms form a surface molecule, which bonds to the indented solid.[11]

In the two-adatom problem, we find that

$$\det(1 - G^0 V) = \det\begin{bmatrix} 1 & -G_{11}^X V_{1a} & 0 & -G_{12}^X V_{2b} \\ -G_{aa}V_{a1} & 1 & 0 & 0 \\ 0 & -G_{21}^X V_{1a} & 1 & -G_{22}^X V_{2b} \\ 0 & 0 & -G_{bb}V_{b2} & 1 \end{bmatrix}$$

$$= (1 - G_{aa}G_{11}^X |V_{1a}|^2)(1 - G_{bb}G_{22}^X |V_{2b}|^2) - G_{aa}G_{12}^X G_{bb}G_{21}^X |V_{1a}|^2 |V_{2b}|^2 \ , \qquad (2.20)$$

the final expression being an algebraic rearrangement after expansion of the determinant by minors. By symmetry, $V_{2b} = V_{1a}$, $G_{bb} = G_{aa}$, $G_{22} = G_{11}$, and $G_{21} = G_{12}$. G_{12} is shorthand for $G_{11,ij}^X(E)$, i.e., 2 denotes the second position ij. Our formulation allows an adatom electron to hop to the nearest solid atom, propagate to the surface atom nearest the second adatom, hop out to this second level, interact, hop back to the solid, propagate, and hop onto the original adatom. We find

$$\det(1 - G^0\hat{V}) = [(1 - G_{aa}G_{11}^X |V_{1a}|^2) - G_{aa}G_{12}^X |V_{1a}|^2] \times [(1 - G_{aa}G_{11}^X |V_{1a}|^2) + G_{aa}G_{12}^X |V_{1a}|^2] \ . \qquad (2.21)$$

Since we are seeking the pair interaction, we must subtract from this expression, which applies to two adatoms on a surface, the $\det(1 - G^0\hat{V})$ for two single noninteracting (i.e., infinitely separated) absorbed atoms. We recall that $V \equiv |V_{a1}|$. If we define $\bar{G}_{aa}^X$ as

$$G_{aa}/(1 - G_{aa}G_{11}^X |V_{1a}|^2) = [E - E_a - V^2 G_{11}^X(E)]^{-1} \ ,$$

then

$$\det(1 - G^0\hat{V})_{\text{pair}} = 1 - (\bar{G}_{aa}^X)^2 (G_{12}^X)^2 V^4 \ ,$$

so that

$$\Delta W_{\text{pair}} = -\frac{2}{\pi}\int_{-\infty}^{E_F} \operatorname{Im}\ln[1 - (\bar{G}_{aa}^X(E))^2 (G_{12}^X(E))^2 V^4]\, dE$$

$$= -\frac{2}{\pi}\int_{-\infty}^{E_F} \operatorname{Im}\ln\left(1 - \frac{V^4 (G_{12}^X(E))^2}{[E - E_a - V^2 G_{11}^X(E)]^2}\right) dE. \qquad (2.22)$$

2. *Commentary*

Equation (2.22) is essentially identical to Grimley's.[4,6] Our $\bar{G}_{aa}$ corresponds to his $G_{A\infty}$ if one rescales our E_a by Un_a or assumes $U = 0$. In Grimley and Walker[6] it is assumed that n_a is replaced by n_∞, the adatom occupation number for single-particle adsorption. Thus, they neglect Grimley's Anderson-model correlation term $\Delta W_2 = -2U(n^2 - n_\infty^2)$,[4] as we do in not treating Coulomb interaction effects explicitly. Their q_A corresponds to our $V^2 G_{11}$ while q_{AB}, $q_{\alpha\beta}$, or q_{st} goes over to our $V^2 G_{12}$, i.e., $V_{a1}G_{12}V_{2b}$. As the matrices in (2.18) and (2.20) illustrate, our perturbation also has no diagonal part. Since $1 - G_{A\infty}^2 q_{st}^2$ is equivalent to our $1 - G_{aa}^2 G_{12}^2 V^4$, we see that our results for $\Delta\rho$ and ΔW_{pair} agree with the results of Grimley and Walker[6] up to a minus sign, which arises from our use of an imaginary infinitesimal of opposite sign to conform to the convention of Kalkstein and Soven.[11] This choice of sign means that the imaginary parts of our Green's functions will have the opposite sign from theirs. Since "Im ln" is just the arctangent of the imaginary part of the argument over the real part, our integrand will have the opposite sign from theirs, canceling the sign discrepancy.

In Grimley and Walker's derivation[6] of the pair-interaction energy (called ϕ_{mix}) in their Appendix, they suggest that the final expression requires the approximation $(\partial/\partial E)G_{A\infty} \cong -G_{A\infty}^2$, at least in the region where the integrand is large. In our language, this approximation becomes $V^2 |(\partial/\partial E)G_{11}| \ll 1$. For physical potentials V, such an approximation is not valid, and our derivation has not required it. In fact, Grimley and Walker's formulas do not require it either, as one might suspect since our answers agree. Their use of the approximation in the appendix cancels an implicit use of it in the text: In their equation (29), $(1/q_{\alpha\beta})(\partial q_{\alpha\beta}/\partial\epsilon)$ should be replaced by $(1/q_{\alpha\beta})(\partial q_{\alpha\beta}/\partial\epsilon) + (1/G_{A\infty}) \times (\partial G_{A\infty}/\partial\epsilon) + G_{A\infty}$.

It should be noted that the approximation that $V^2 G_{11}(E)$ can be replaced by a complex constant

appears in most applications of the Anderson model. In particular, it is used in the original paper[8] and most subsequent treatments of two bulk impurities.[12,13] In fact, there is evidence that the approximation is not always valid in the bulk-impurity problem.[14] Except for weak binding[7] the approximation is invalid for the problem considered here. In the localized moment or divacancy problem, one assumes that the free-electron-like s bands are dominant. In chemisorption, the interaction between the "impurities," i.e., adatoms, is mediated by d-like electrons, which are better represented by a tight-binding model. The treatments of two close bulk impurities[12] further assume that the interaction propagating term $V^2G_{12}(E)$ is a complex constant or, equivalently, that it is overshadowed by a constant direct interaction term. Such an assumption would clearly be unreasonable in the present study, except in certain cases of unphysically weak binding.

It is usually a reasonable approximation (although we shall not need to make it in our actual calculations) to take $|G_{aa}^2G_{12}^2V^4| \ll 1$ and hence write

$$\Delta W_{\text{pair}} = \frac{2}{\pi}\int_{-\infty}^{E_F} \operatorname{Im}\frac{V^4(G_{12}^X)^2}{(E-E_a-V^2G_{11}^X)^2}\,dE \quad . \tag{2.23}$$

This expression is analogous to the first-order expression derived by Kim and Nagaoka[15] for two bulk impurities. If we assume $V^2G_{11}(E) = \alpha + i\Gamma$ and $V^2G_{12}(E) = \beta + i\Delta$ to be independent of energy (an extremely poor approximation for us), as in Grimley (Secs. 3 and 4)[4] (except that our Γ and Δ have the opposite sign from his, so that Γ is always positive), then

$$\Delta W = -\frac{2}{\pi}\operatorname{Im}\frac{V^4G_{12}^2}{E_F-E_a-V^2G_{11}} = -\frac{2}{\pi}\operatorname{Im}\frac{(\beta^2-\Delta^2)+i2\beta\Delta}{(E_F-E_a-\alpha)-i\Gamma} \quad . \tag{2.24}$$

In the case (Grimley's Sec. 4.1[4])

$$|E_F-E_a-\alpha| \equiv |E_F-E_V| \ll \Gamma \ll E_V \quad ,$$

we see that

$$\Delta W \to -\frac{2}{\pi}\frac{\beta^2-\Delta^2}{\Gamma} \quad ,$$

which differs from Grimley's[4] Eq. (34) for this case, with $U=0$. Careful expansion of Grimley's functions f shows that

$$\Delta W_1 = \frac{4\beta\Delta E_V}{\pi\Gamma^2} + \frac{2(\Delta^2-\beta^2)}{\pi\Gamma} + [\text{higher-order terms in } \Gamma/E_V \text{ or } (E_V-E_F)/\Gamma]\,; \tag{2.25}$$

in Grimley's paper, 8 incorrectly appears instead of 4. Hence, with $U=0$,

$$\Delta W = \Delta W_1 + \Delta W_3 = \frac{2\beta\Delta}{\pi\Gamma^2}(2E_V-2E_F) + \frac{2(\Delta^2-\beta^2)}{\pi\Gamma} \approx -\frac{2}{\pi}\frac{\beta^2-\Delta^2}{\Gamma} \quad , \tag{2.26}$$

since $|E_V-E_F|/\Gamma$ is small. Indeed, Grimley's expression, which is proportional to $(4E_V-2E_F)$, is physically unreasonable since it depends on the zero of energy.

In the case (Grimley's Sec. 4.2[4]) that $|E_V-E_F| \gg \Gamma \ll |E_V|$, our simple expansion suggests

$$\Delta W = -\frac{4}{\pi}\frac{\beta\Delta}{E_F-E_V} \quad ,$$

while Grimley's expansion gives (after a bit of algebra)

$$\Delta W = -\frac{4}{\pi}\frac{\beta\Delta}{E_F-E_V}\frac{E_F}{E_V} \quad ,$$

which essentially agree for $|E_F-E_V| \ll E_V$. Only in this limit does Grimley's expression satisfy independence of the energy origin, a general consequence of electron conservation.

As Grimley and Walker (Appendix I)[6] note, the interaction energy goes to zero as the Fermi energy approaches $+\infty$. (If there are no split-off states, then it vanishes for a filled band.) This very general result is one of the few checks one has when performing actual numerical calculations. In essence, it arises from the fact that our perturbing potential is purely off diagonal in the site representation. Hence $\operatorname{Tr}\mathcal{H} = \operatorname{Tr}\mathcal{H}_0$; that is, there is no interaction energy (difference in energy from the unperturbed case) if all band levels are occupied, even though individual levels may shift. Since this result is of such importance and utility, we will present short explicit proofs for the single- and pair-adatom cases. Both rely on the fact that all the poles of the Green's functions are in the upper half of the complex energy plane.

For single-atom adsorption, we consider the integral (2.19),

$$\Delta W = -(2/\pi)\int_{-\infty}^{\infty} \operatorname{Im}\ln[1-G_{aa}(E)G_{11}^X(E)V^2]\,dE \quad ,$$

where $G_{aa}(E) = (E-E_a-i\delta)^{-1}$ and

$$G_{11}^X(E) = \sum_k \frac{|\langle 1|k\rangle|^2}{E-E_k-i\delta} \quad ,$$

where $|k\rangle$ are the eigenstates and the eigenvalues of the unperturbed Hamiltonian, and $|1\rangle$ is the binding-site vector (possibly a symmetrical combination of a few surface positions). An integration by parts gives

$$\Delta W = -\frac{2}{\pi}E\operatorname{Im}\ln[1-G_{aa}(E)G_{11}^X(E)V^2]\Big|_{-\infty}^{\infty} - \frac{2}{\pi}\operatorname{Im}\int_{-\infty}^{\infty} E\left(\frac{V^2G_{11}^X(E)}{(E-E_a-i\delta)^2}\right.$$

$$+V^2G_{aa}(E)\sum_k \frac{|\langle 1|k\rangle|^2}{(E-E_k-i\delta)^2}\Bigg) \times \frac{dE}{1-G_{aa}(E)G_{11}^X(E)V^2} \quad . \quad (2.27)$$

The surface term vanishes since for any energy outside the band, the argument of the log is pure real. Hence the term vanishes for large but finite E, and therefore also in the limit $E \to \pm\infty$. The second term can be made into a contour integral and closed in the lower half-plane of the energy plane, where there are no poles. [Note $(1-V^2G_{aa}G_{11})^{-1}$ essentially has the properties of $(E-E_a-V^2G_{11}^X)^{-1}$, and $\mathrm{Im}G_{11}^X \gtrless 0$ by remark (vii), so the poles are also in the upper half-plane.] Since the integrand approaches E^{-2} asymptotically, the semicircular path vanishes, and the integral must be zero. Hence $\Delta W = 0$.

Similarly for the two-atom case, we integrate

$$\Delta W = -(2/\pi)\int_{-\infty}^{\infty} \mathrm{Im}\ln(1-G_{aa}^2G_{ij}^2V^4)\,dE$$

by parts. The surface term vanishes as above, so that

$$\Delta W = \frac{2}{\pi}\int_{-\infty}^{\infty} E\,\mathrm{Im}\frac{\partial}{\partial E}(V^4G_{aa}^2G_{ij}^2)\frac{dE}{1-G_{aa}^2G_{ij}^2V^4} \quad . \quad (2.28)$$

Again it is easy to show that the derivative term is analytic in the lower half-plane. Also,

$$1-G_{aa}^2G_{ij}^2V^4 = \frac{[E-E_a-V^2(G_{11}^X+G_{ij}^X)][E-E_a-V^2(G_{11}^X-G_{ij}^X)]}{(E-E_a-V^2G_{11}^X)^2} \quad . \quad (2.29)$$

By remarks (viii) and (vii), the positive $\mathrm{Im}G_{11}^X(E)$ dominate $\mathrm{Im}G_{ij}^X(E)$, so that its zeros are above the real axis. Again, then, we can close below to obtain the vanishing of the integral.

3. *Analysis of Split-Off States*

Finally, we come to split-off states, sharply localized energy states lying above or below the band. In the case of single-adatom adsorption, one is manifested by a zero of $E-E_a-V^2\mathrm{Re}G_{11}^X(E)$ outside the band. In the pair problem, $E-E_a-V^2\times(\mathrm{Re}G_{11}^X \pm \mathrm{Re}G_{ij}^X)$ vanishes outside the band. The following observations will aid our analysis: Remark (vii) indicates that for any binding position the imaginary part of the "self," or 11, Green's function is positive throughout the band [and vanishes outside, by remark (v)]. Hence, since the Green's function satisfies a Kramers–Kronig relation [written down in remark (v); the range of integration need only extend over the band to pick up all contributions to ReG], we find that $|\mathrm{Re}G_{11}^X(E)|$ must be monotonically decreasing outside the band as $|E|$ increases. Moreover, with our choice of sign for the imaginary infinitesimal $i\delta$, we have that positive imaginary G_{11} implies that $\mathrm{Re}G_{11}^X(E)$ is positive above the band and negative below.

Now below the band $E-E_a$ is negative, presuming E_a to be within the band. The above observations indicate that $-V^2\mathrm{Re}G_{11}^X(E)$, i.e., $V^2|\mathrm{Re}G_{11}^X(E)|$, decreases as E becomes more negative. Hence

$$f(E) = E-E_a-V^2\,\mathrm{Re}G_{11}^X(E)$$

is a decreasing function below the band as the energy E becomes more negative. For small V, $f(E)$ will be negative at the band edge, and merely increase in magnitude as E separates farther from the bottom of the band. For large potential, however, it will be positive at the lower edge. As E approaches $-\infty$, $f(E)$ approaches E and is negative. Since $f(E)$ is continuous and monotonically decreasing, it must have a single zero below the band, which we denote by E_S. Thus,

$$E_S-E_a-V^2\,\mathrm{Re}G_{11}^X(E_S)=0\ , \quad E_S < -\tfrac{1}{2}W_b \quad . \quad (2.30)$$

Similarly, there can be at most one such split-off energy above the band. This discussion parallels Newns's[7] graphical analysis and applies to any case where the change in density of states (i.e., the spectral-weight function) is positive throughout the band.

In determining the contribution of a split-off state to $\Delta W_{\text{single}}^X$, it is convenient to write (2.19) as

$$\Delta W_{\text{single}}^X = (2/\pi)\Big\{\int_{-\infty}^{E_F}\mathrm{Im}\ln\,(E-E_a-i\delta)\,dE - \int_{-\infty}^{E_F}\mathrm{Im}\ln[E-E_a-V^2G_{11}^X(E)-i\delta]\,dE\Big\} \quad , \quad (2.31)$$

which is the form in which the actual computer computation is made. Within the band, the $i\delta$ of the second term is unimportant since $\mathrm{Im}G_{11}^X(E)$ is positive. Below the band, $i\delta$ gives the only imaginary part, so that the integrand of either term is $-\pi$ (0) if the real part of the argument of the natural logarithm is negative (positive). For all E below the band, the integrand of the first term is $-\pi$. For E sufficiently below the band, $E-E_a-V^2\mathrm{Re}G_{11}^X(E)$ will also be negative, so that the two integrals cancel for E sufficiently negative. This cancellation eliminates any difficulty at $-\infty$. If there is a split-off state, then between E_S and E_0, where E_0 is the energy of the bottom of the band (i.e., $-\frac{1}{2}W_b$), the integrands do not cancel, and we find a contribution of $(2/\pi)(-\pi)(E_0-E_S)$, or $2(E_S-E_0)$, to ΔW^X. Equation (2.19) can be written

$$\Delta W_{\text{single}}^X = 2(E_S-E_0) - \frac{2}{\pi}\int_{E_0}^{E_F}\mathrm{Im}\ln\left(1-\frac{V^2G_{11}^X(E)}{E-E_a-i\delta}\right)dE \quad (2.32)$$

if we set $E_S = E_0$ when no split-off state exists below the band.

As was noted above, the integral term of (2.32) approaches a constant in V. Hence as the potential becomes very large $\Delta W^X_{\text{single}} \sim 2E_S(V)$. In this region $|E_S| \gg |E_0|$, so that we are in the asymptotic region of the Green's function, where

$$\mathrm{Re}G^X_{11}(E) \sim (1/\pi E)\int_{E_0}^{|E_0|} \mathrm{Im}G^X_{11}(E')\,dE' = 1/E \quad ,$$

where the equality holds for any binding type and reflects the addition of the single-adatom electron to the system. In this region, (2.30) reduces to a quadratic equation with the solution

$$E_S = \tfrac{1}{2}[E_a - (E_a^2 + 4V^2)^{1/2}] \quad . \tag{2.33}$$

Thus, as V grows very large, E_S approaches $-V$, so that $\Delta W(V) \sim -2V$.

A state split off above the band can be treated in similar fashion. Such a state must be included if the trace theorem proved just above that $\Delta W = 0$ as E_F grows large (or merely at $E_F = |E_0| = \frac{1}{2}W_b$ if there is no split-off state above the band). Since we restrict the Fermi energy to be within the band, this upper state is unimportant in our computation.

In the case of the pair interactions, the inclusion of split-off states is more complicated, but not more difficult. As suggested by (2.29), it is convenient to decompose (2.22) as

$$\Delta W^X_{ij} = -(2/\pi)\int_{-\infty}^{E_F} dE\,(\mathrm{Im}\ln\{E - E_a - V^2[G^X_{11}(E) + G^X_{ij}(E)] - i\delta\} + \mathrm{Im}\ln\{E - E_a - V^2[G^X_{11}(E) - G^X_{ij}(E)] - i\delta\} - 2\,\mathrm{Im}\ln\{E - E_a - V^2 G^X_{11}(E) - i\delta\}) \quad . \tag{2.34}$$

Again, the imaginary infinitesimals are important only outside the band. By remark (viii), $\mathrm{Im}G^X_{11}(E) \mp \mathrm{Im}G^X_{ij}(E)$ is non-negative throughout the band. Hence, as in the single-adatom problem, the Kramers–Kronig relation indicates that $\mathrm{Re}G^X_{11}(E) \mp \mathrm{Re}G^X_{ij}(E)$ is positive above the band, negative below it, and monotonically decreasing in magnitude with increasing $|E|$ (outside the band). For sufficiently large $|E|$, the real parts of all three arguments will be negative. Each will contribute an integrand of $-\pi$, leading to cancellation. For sufficiently strong potential, however, the real parts will become positive below the lower band edge. Let $E_\pm$ be defined by

$$E_\pm - E_a - V^2[\mathrm{Re}G^X_{11}(E_\pm) \pm \mathrm{Re}G^X_{ij}(E_\pm)] = 0 \ , \quad E_\pm < E_0 . \tag{2.35}$$

Then it is clear from the single-adatom problem that the contribution of split-off states to the pair-interaction energy is

$$-(2/\pi)(\pi)[(E_0 - E_+) + (E_0 - E_-) - 2(E_0 - E_S)]$$

when E_F is within the band. Thus we can rewrite (2.22) as

$$\Delta W^X_{ij} = 2(E_+ + E_- - 2E_S) - (2/\pi)\int_{E_0}^{E_F} \mathrm{Im}\ln[1 - V^4(G^X_{aa})^2(E)(G^X_{ij})^2(E)]\,dE \quad , \tag{2.36}$$

again with the understanding that if there is no zero below the band in any one of the three real parts in the arguments in (2.34), the corresponding $E_\pm$ or E_S is taken to be E_0, so that in the event of no splitting off, the first term of (2.36) vanishes. Recall from remark (v) that $\mathrm{Re}G^X_{ij}(E_0)$ is negative. Hence, as potential decreases, E_- will be the first split-off state to disappear (enter the band), followed by E_S, and finally E_+.

Finally, we examine the asymptotic form of $\Delta W^X_{ij}(V)$. As suggested by the factorization of (2.29), as V becomes very large, the integral term of (2.36) becomes independent of V, with the value

$$-\frac{2}{\pi}\int_{E_0}^{E_F} dE\,\mathrm{Im}\ln\left(1 - \frac{(G^X_{ij}(E))^2}{(G^X_{11}(E))^2}\right) .$$

To analyze the split-off-state term, we must write ReG in terms of a moment expansion:

$$\mathrm{Re}G \sim \frac{1}{E}\sum_{n=0}^{\infty}\frac{\mu_n}{E^n} \quad \text{for } |E| > |E_0|$$

where

$$\mu_n = (1/\pi)\int_{E_0}^{|E_0|} (E')^n \mathrm{Im}G(E')\,dE'$$

is called the nth moment. Now for atop binding ($X = A$), μ_0 is finite (and equal to unity) only for $(ij) = (11)$. Since $G^B_{11} = G^A_{11} + G^A_{12}$ and $G^C_{11} = G^A_{11} + 2G^A_{12} + G^A_{22}$, μ_0 is unity for all X when $(ij) = (11)$. For (ij) not equal to (11), the zeroth moment of $\mathrm{Im}G^X_{ij}$ vanishes in general. There are three exceptions to this statement: G^B_{12}, G^C_{12}, and G^C_{22}. The source of the exception is that the two adatoms share the surface atom between them as a nearest neighbor. In the formalism, this is manifested by the presence of G^A_{11} as a component, e.g., $G^B_{12} = G^A_{12} + \frac{1}{2}(G^A_{11} + G^A_{13})$. In these special cases we need not go to higher moment to find the contribution of the split-off states. Solving (2.30) and (2.35) for large V, we easily find that

$$2(E_+ + E_- - 2E_S) \approx -2V[(1+\tilde{\mu})^{1/2} + (1-\tilde{\mu})^{1/2} - 2],$$

where $\tilde{\mu}$ is the zeroth moment of $\mathrm{Im}G^X_{ij}$, or equivalently the coefficient G^A_{11}, e.g., $\tilde{\mu} = \frac{1}{2}$ for G^B_{12}. The physical ramification of this special case is the growth of a surface macromolecule rather than merely an island composed of dimers. However, in this case the direct interaction may also be important and must be added on in any detailed calculation of the energy of the configuration.

In general, however, $\Delta W^X_{ij}(V)$ is not asymptotically linear in V. In fact, $\Delta W(V)$ approaches the constant determined by the limit of the integral term in (2.36)! The split-off states give a net

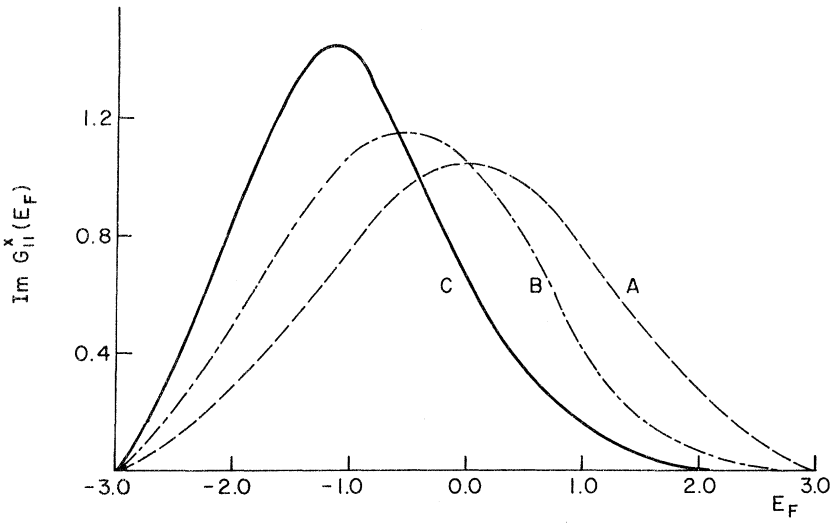

FIG. 3. Imaginary part of the "self" (11) Green's function, or π times the change in the density of states, at a binding site for atop (A), bridge (B), and centered (C) binding. The curves verify the downward shift in energy of the symmetrized surface Wannier states The implicit energy unit used throughout is twice the tight-binding hopping matrix strength, i.e., $2T$, or equivalent one-sixth the bandwidth.

contribution of order $1/V$ in this region if $\mathrm{Im}G_{ij}^X$ has a nonvanishing first moment μ_1. [That is, $E_+ + E_- - 2E_S \approx -\frac{5}{4}(\mu_1^2/V)$.] If $\mathrm{Im}G_{ij}^X(E)$ is even in E, then the split-off contribution is even higher order in $1/V$.

III. CALCULATION RESULTS

A. Single Atom Adsorption

As noted earlier, the implicit energy unit of our calculation is $2T$, i.e., $\frac{1}{6}W_b$, the natural unit of the tight-binding model. We evaluate numerically the integral

$$\Delta W^X = -\frac{2}{\pi}\int_{E_0}^{E_F} \mathrm{Im}\ln\left(1 - \frac{V^2 G_{11}^X(E)}{E - E_a - i\delta}\right) dE + \begin{cases} 2(E_S - E_0) \\ 0 \end{cases}, \quad (3.1)$$

where $X = A$ (atop), B (bridge), or C (centered); BP (bridge-perpendicular) is redundant to B. The second term is nonzero when a split-off state of energy E_s lies below the lower band edge $E_0 \equiv -\frac{1}{2}W_b$; E_s is determined by Eq. (2.30). For homonuclear diatomic adsorbates, the single-particle interaction energy ΔW is minus one-half of the sum of the heat of adsorption and the dissociation energy of the molecule. We note that

$$G_{11}^B(E) = G_{11}^A(E) + G_{12}^A(E)$$

and

$$G_{11}^C(E) = G_{11}^A(E) + 2G_{12}^A(E) + G_{22}^A(E) \ . \quad (3.2)$$

From remarks (ii), (iii), (v), and (vi) concerning the $G_{ij}^A(E)$, or from direct computation, we have (a) $\mathrm{Im}G_{11}^A(E)$ is symmetric and positive, with a single extremum in the middle of the band; (b) $\mathrm{Im}G_{12}^A(E)$ is antisymmetric, with its positive peak in the lower half of the band; (c) $\mathrm{Im}G_{22}^A(E)$ is symmetric, with a negative bulge around the center of the band, and a positive extremum toward each end. Thus, $\Delta\rho^B = (1/\pi)\mathrm{Im}G_{11}^A(E)$ is skewed into the lower half of the band, lowering the average electron energy, as one would expect of a bonding state. This effect is even more pronounced for $\Delta\rho^C$, where all three addends combine constructively near the bottom of the band, while $2G_{12}^A$ competes with $G_{11}^A + G_{22}^A$ near the top (see Fig. 3). In essence we are saying that ρ peaks at lower energy for non-atop binding because the adatom's electron mixes with a suitably phased combination of orbitals on the nearest neighbors in the substrate surface, resulting in only plus signs in Eq. (3.2).

We compute ΔW for E_a, the adatom noninteracting level, at and near the center of the band, and at $\frac{1}{4}W_b$ from each edge. The Fermi energy sweeps through the band in increments of 0.1. We have carried out computations on adatom-surface couplings of the following strengths: $V/T = 1$, 2, 3, 4, 5, 6; that is, V/W_b in the range $\frac{1}{12}$–$\frac{1}{2}$. For $V/T = 5$ or 6, and often for weaker potential ($V/T = 4$), when E_a is far from the band center, one finds split-off states of energy E_S.

Our calculation of ΔW^X revealed the general structure (cf. Fig. 4) of an inverted triangle (the base being the E_F axis), smoothed at the base edges. Starting at zero (when there is no split-off state) at the lower edge, ΔW begins falling with increasing E_F (within a range of about $\frac{1}{10}W_b$, depending on V), soon becoming linear until it reaches its largest (negative) value when $E_F = E_a$. In essence, $|\Delta W|$ is maximum when $E_F \simeq E_a$ because in this case the maximum number of electrons have their energies lowered with few electrons having their energies raised (i.e., the lower half of the

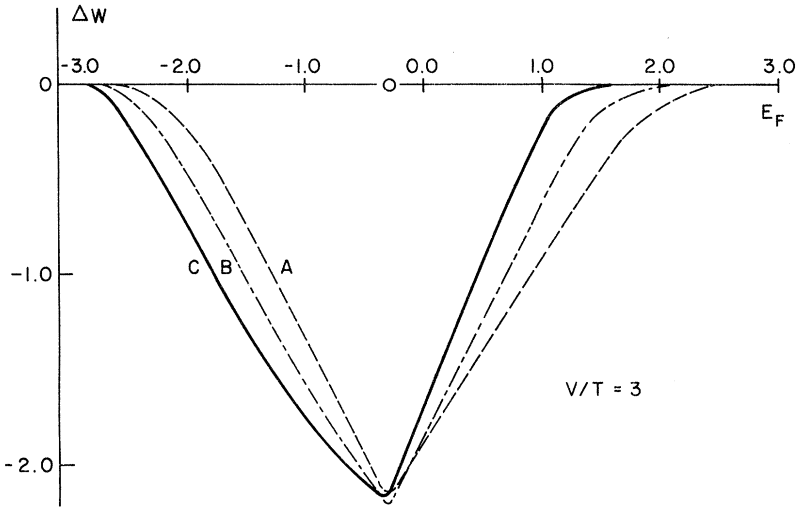

FIG. 4. Interaction energy for the adsorption of a single atom. E_a, denoted by the small circle on the abscissa, is -0.3. A, B, and C denote atop, bridge, and centered binding, respectively.

virtual level is occupied, the upper half is empty). Alternatively, the adatom level is broadened by the interaction with the substrate; when it is half-filled, electrons take optimal advantage of this broadening, $|\Delta W|$ then decreases linearly and smoothly vanishes near the top of the band. There are no positive (repulsive) peaks and no noticeable substructure. If one assumes V is the same for all binding types, then invariably ΔW^C begins falling first, followed by ΔW^B, and ΔW^A trailing; similarly, they follow the same order in rising toward the axis. Thus, when E_F is not too near E_a, one has $|\Delta W^C| > |\Delta W^B| > |\Delta W^A|$ for $E_F < E_a$ and $|\Delta W^C| < |\Delta W^B| < |\Delta W^A|$ for $E_F > E_a$. This is in accord with the observation that $\Delta\rho$ for centered binding is most strongly skewed downward in energy, with the change in density of states for bridge binding skewed moderately, and the atop $\Delta\rho$ not skewed at all.

When a state has split off below or above the band, the interaction energy curve is negative at the appropriate band edge rather than going to zero there (cf. Fig. 5). The other qualitative features of the curve remain the same. Hybridization skewing dictates that a state splits off below the band for C binding first (as V increases), then B, and finally A, assuming the same V for each binding type. At a given potential, the magnitude of the split-off energy, and hence the absolute value of ΔW at the lower edge, will be greatest for C, weakest for A. For states split off above the band, the symmetry order naturally reverses: A splits off first and most strongly, and so on.

Recently, Messmer and Bennett[16] have proposed an extension of the Woodward–Hoffman symmetry rules of reaction chemistry to the problem of

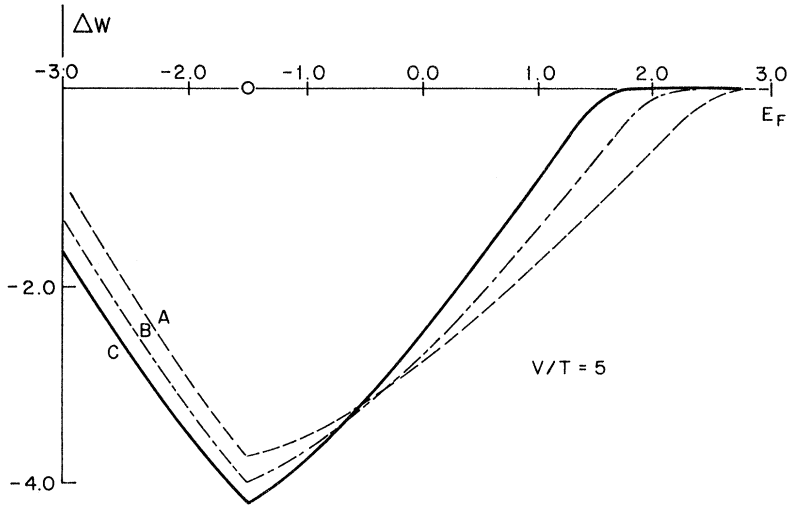

FIG. 5. Interaction energy for the adsorption of a single adatom. $E_a = -1.5$. A (doubly occupied) state has split off below the band for each of the three binding symmetries.

chemisorption. They argue that the binding energy is determined primarily by the matching of the symmetry of the adsorbate orbital and the substrate orbitals of energy equal to E_F. Our results suggest a more involved picture in that the binding comes from states throughout the band, with states near E_F and/or E_a playing a dominant role only when $E_a \simeq E_F$ and V is small.

Hybridizing also accounts for the following phenomena: For E_a near the center of the band, the spread among the three ΔW^X $(E_F = E_a)$ relative to their average is quite small, on the order of a few percent. (This percentage decreases as V increases.) For $E_a = -1.5$, $|\Delta W^C\ (E_F = E_a)| > |\Delta W^B| > |\Delta W^A|$, the relative spread ranging from 35 to 13% (as V increases). Correspondingly, for $E_a = +1.5$, $|\Delta W^A (E_F = E_a)| > |\Delta W^B| > |\Delta W^C|$, with an even greater spread (50–24%). For $E_a = -1.5$, -0.3, and 0.0, the average maximum binding energy, $\frac{1}{3}[\Delta W^A(E_a) + \Delta W^B(E_a) + \Delta W^C(E_a)]$ is about the same, to within a few percent, with $E_a = -0.3$ consistently highest and $E_a = -1.5$ least in magnitude. The average binding at $E_F = E_a = +1.5$ is only about $\frac{3}{4}$–$\frac{7}{8}$ the strength at the other three adatom-level values.

For most of our range of hopping potential, the interaction lies well between the perturbation regime $(\Delta W \propto V^2)$ and the surface-molecule limit $(\Delta W \propto V)$. If we try to fit the data with a relation $\Delta W(E_a) \propto (V/T)^\alpha$, we see that α increases (within the range 1–2) as V decreases or as E_a moves into a region of relatively weaker binding. In the case of largest V/T, we find ourselves quite near the surface-molecule extreme $\alpha = 1$. We also find here the familiar result that the interaction energy increases as the band narrows: Since both ΔW and V are scaled by T, and thus W_b, $\Delta W \propto W_b^{1-\alpha}$. In the surface-molecule limit, ΔW becomes independent of the bandwidth, so that the band appears to the adatom as essentially a single energy level.

The maximum binding energy (averaged over $X = A, B, C$) at $E_a = 0.0$, -0.3, or -1.5, is roughly $\frac{1}{3}$, $\frac{1}{2}$, $\frac{2}{3}$, or $\frac{5}{6}$ the bandwidth for $V/T = 3$, 4, 5, or 6, respectively. The data in Table I suggest a ratio of binding energy to bandwidth of about $\frac{1}{3}$–$\frac{2}{3}$. Thus, within our model, we obtain agreement with experiment when the hopping matrix element between adatom and substrate atom is about three to six times that between substrate atoms.

B. Pair Interaction

To obtain the pair-interaction energy, i.e., the energy difference between two atoms adsorbed at nearby sites and two adatoms infinitely separated, (Table II), we must compute the integral

$$\Delta W_{ij}^X = -\frac{2}{\pi}\int_{E_0}^{E_F} \mathrm{Im}\ln[1 - V^4(G_{aa}^X(E))^2 (G_{ij}^X(E))^2]dE + \begin{cases} 2(E_+ + E_- - 2E_s) \\ 0 \end{cases}, \quad (3.3)$$

where

$$\bar{G}_{aa}^X(E) = G_{aa}(E)/[1 - V^2 G_{aa}(E) G_{11}^X(E)] .$$

The second term is nonzero when there are split-off states below the band. E_s is given by Eq. (2.30), $E_\pm$ by Eq. (2.35). When a particular state has not split off, it is replaced by E_0 in Eq. (3.3). We find a structure much richer than for single-atom adsorption. Again we compute with the parameters $E_a = -1.5$, -0.3, 0.0, and $+1.5$ or $+2.0$; $V/T = 1$, 2, 3, 4, 5; and E_F in steps of 0.1. The interaction is computed for eight values of (ij): (12), (22), (13), (33), (14), (15), and (16). With the aid of the symmetries of remark (iv), we know the interaction strength at the 24 lattice points (excluding the origin) within or on the boundary of a square of side $5a_0$ centered at the origin, i.e., at points less than $2.9a_0$ away from the origin point. In a ⟨10⟩ direction we know ΔW for points as far as $5a_0$. In order to improve accuracy, we also linearly interpolate Green's functions and then calculate the integral in steps of 0.05 rather than 0.1.

For the calculation of split-off states, steps of 0.025 were used within 0.2 of the band edges, since when a state is about to split off from the band, violent oscillations often occur there. Moreover, for large V it proved advisable to linearly approximate the Green's functions and to thereby evaluate an exact integral over a mesh spacing rather than performing a trapezoidal-rule summation. The sum rule given at the end of Sec. II B is generally reasonably well satisfied, except for the more distant points and stronger potentials. In the latter circumstance, often states are splitting off only below the band, and the most rapid oscillations occur near the lower edge. Here it becomes very desirable to integrate down from the top of the band, as permitted by the sum rule.

In this calculation, split-off states occur for weaker potentials than for the single-atom case, as in suggested by the factorization

$$1 - V^4(G_{aa}^X(E))^2 (G_{ij}^X(E))^2 = \frac{(E - E_a - V^2 G_{11}^X - V^2 G_{ij}^X)(E - E_a - V^2 G_{11}^X + V^2 G_{ij}^X)}{(E - E_a - V^2 G_{11}^X)^2}, \quad (3.4)$$

where the first factor in the numerator represents the downward-shifted state and the second term the upward-shifted one (cf. Grimley[4]). For $E_a = -1.5$, splitting off occurs for $V/T \gtrsim 3$. For $E_a = +1.5$, it just begins to happen at $V/T = 3$. With E_a near the center of the band, split-off states appear when $V/T = 4$.

In the pair problem we find a more dramatic

dependence on potential than in the single-atom case. For $V/T=1$, the strongest interaction occurs for $E_F=E_a$, with a spread of about $\frac{1}{6}W_b$ in each direction (less for $E_a=-1.5$). It is characterized by one or two pronounced crests and troughs in ΔW_{ij}^X (see Fig. 6). For $V/T=2$, the interaction is scarcely localized, but still largest near $E_F=E_a$. (With $E_a=-1.5$, the strong variation of the interaction energy is still largely confined to the lower half of the band; by $E_F=1.0$, the interaction fades away.) When $V/T=3$ there appears to be no localization within the energy band, and one begins to see the precursor(s) of split-off states (cf. Fig. 7). Such precursor states are characterized by a narrow pronounced oscillation of the interaction-energy curve near a band edge. For $V/T=4$, splitting off has begun (i.e., for E_a in the lower half or middle of the band, at least the state corresponding to $G_{11}^X+G_{ij}^X$ has fallen below the lower band edge; for E_a well into the upper half, a similar state has split from the upper edge). For $V/T=5$ or 6, splitting off is generally com-

TABLE I. Tabulation of data used in estimating the adatom-surface atom hopping parameter V. The energy of binding a single adatom to a surface, $-\Delta W$, is obtained readily from experiment. The [d-] band width of the substrate can be extracted crudely from band-structure computations. By comparing the ratio of $-\Delta W/W_b$ thus obtained with calculations based on the present model, we fix $V/T\cong 3$–5 to describe chemisorption.

Substrate	Crystal structure	W_b (eV)[a]	Adsorbate	$-\Delta W$ (eV)[b]	$-\Delta W/W_b$
W	bcc	10.5(14.1)[c]	H	3.2	$\frac{1}{3}$
			O	6.8	$\frac{2}{3}$
			N	7.0	$\frac{2}{3}$
			CO	3.6	$\frac{1}{3}$
Mo	bcc	9.2[c]	H	3.1	$\frac{1}{3}$
			O	6.3	$\frac{2}{3}$
Cr	bcc	6.9[c]	H	3.2	$\frac{3}{7}$
Fe	bcc	6.0[d]	H	3.0	$\frac{1}{2}$
			N	6.4	1
			CO	2.0	$\frac{1}{3}$
Ni	fcc	4.6[e]	H	2.9	$\frac{5}{8}$
			CO	1.8	$\frac{2}{5}$
Rh	fcc	6.44[f]	H	2.9	$\frac{3}{7}$
			O	5.1	$\frac{4}{5}$
Pd	fcc	5.08[f]	H	2.8	$\frac{4}{7}$
			O	4.0	$\frac{4}{5}$
Pt	fcc	7.16[f]	O	4.1	$\frac{4}{7}$

[a]These bandwidth values are based on augmented-plane-wave calculations. For bcc substrates, the d-band width is taken to be the energy difference $E(H_{25'})-E(H_{12})$; for fcc substrates, it is estimated by $E(L_2')-E(L_1)$. Since the representation of an actual d-band by a single tight-binding band is very approximate, these values should be considered to give the bandwidth to one significant figure at best.

[b]Experimental heats of chemisorption for diatomic gases from D. O. Hayward and B. M. W. Trapnell, *Chemisorption* 2nd ed. (Butterworth, London, 1964), pp. 203–4. Dissociation energies for H_2, O_2, and N_2 from *Handbook of Chemistry and Physics*, 44th ed., edited by Charles D. Hodgman *et al.* (Chemical Rubber Publishing Co., Cleveland, 1962), p. 3519.

[c]L. F. Mattheiss, Phys. Rev. 139, A1893 (1965). For tungsten, two results are given, corresponding to slightly different crystal potentials. It is suggested that the first smaller value is the more accurate prediction of the actual 5d bandwidth of W.

[d]J. H. Wood, Phys. Rev. 126, 517 (1962).

[e]L. Hodges, H. Ehrenreich, and N. D. Lang, Phys. Rev. 152, 505 (1966), citing J. G. Hanus, MIT Solid State and Molecular Theory Group Quarterly Progress Report No. 44, 29 (1962) (unpublished).

[f]O. Krogh Andersen, Phys. Rev. B 2, 883 (1970), a relativistic calculation.

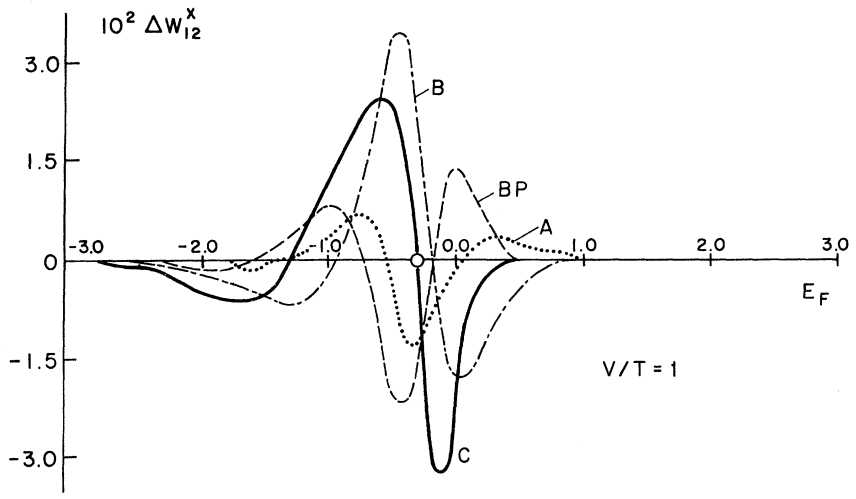

FIG. 6. Nearest-neighbor pair-interaction energy for weak potential (equal to the tight-binding hopping constant); $E_a = -0.3$. In this and subsequent figures, A, C, B, and BP denote atop, centered, bridge, and bridge-perpendicular, respectively.

pleted from one edge (e.g., even the $G^X_{11} - G^X_{ij}$ state has separated), and precursors or actual splitting off is beginning at the other band edge, as in Fig. 8. For the stronger potentials ($V/T = 3$ or 4, or more), the curving of ΔW^X_{ij} is no longer so sensitive to V, especially away from the edges; increased potential tends to scale up (and possibly slightly shift) the curves. This discussion is capsulized in Fig. 9, which shows the effects of increasing V while holding the other parameters fixed: we see (a) state split off below the band and (b) little difference (for stronger V) in the shape of the curves in the band interior.

Also unlike the single-atom case, we find many smoothly peaked extrema of ΔW as E_F varies over the band. The number of extrema of ΔW^X_{ij} is greater (often by as much as a factor of 2) than the number of extrema of $\mathrm{Im}G^A_{ij}$, as given in remark (vi), except apparently for some types of binding at the distant sites—$(ij) = (15)$ or (16), a distance $> 3.5a_0$ from the origin—although in these cases there are so many bumps of small magnitude that some may be smothered by the finite mesh size. Almost always, atop binding has the greatest number of extrema in the energy band, while centered binding has the fewest, the difference being of the order of a quarter of the total number. Conversely, the centered extrema are usually greatest in magnitude while the atop are smallest. Bridge binding tends to track-centered binding, especially for near sites toward the $\langle 10 \rangle$ direction—$(ij) = (12)$, (13), and (23), a distance $< 2.5a_0$ from the origin; also in this region, bridge perpendicular tracks atop. By tracking, we mean that two curves have the same, or nearly the same, number of extrema of comparable relative height, but often displaced

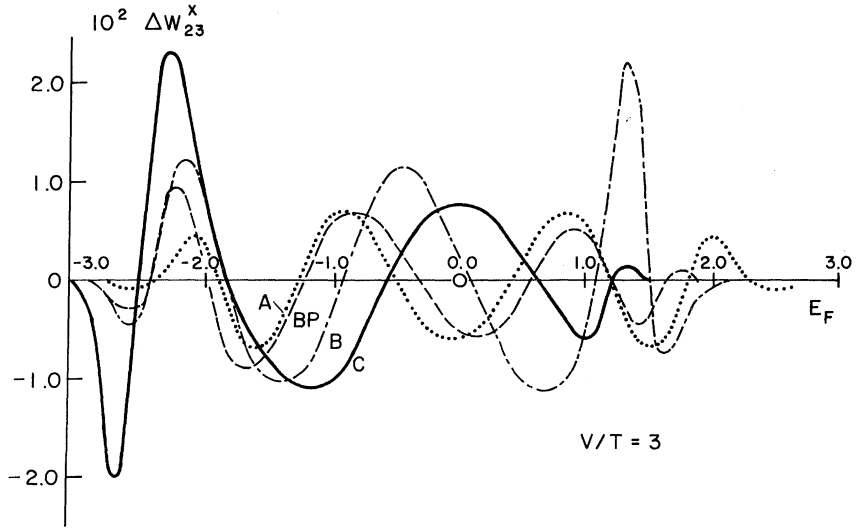

FIG. 7. Pair-interaction energy for fourth-nearest neighbors with a potential not quite strong enough to split off states; $E_a = 0.0$. Note that (i) the interaction is much less localized within the band than in Fig. 6; (ii) the energy scale of the ordinate is similar to that in Fig. 6, indicating that the effect on $|\Delta W|$ of the increase in potential is compensated by the increase in interaction distance; and (iii) the precursors of split-off states are beginning to emerge near the band edges.

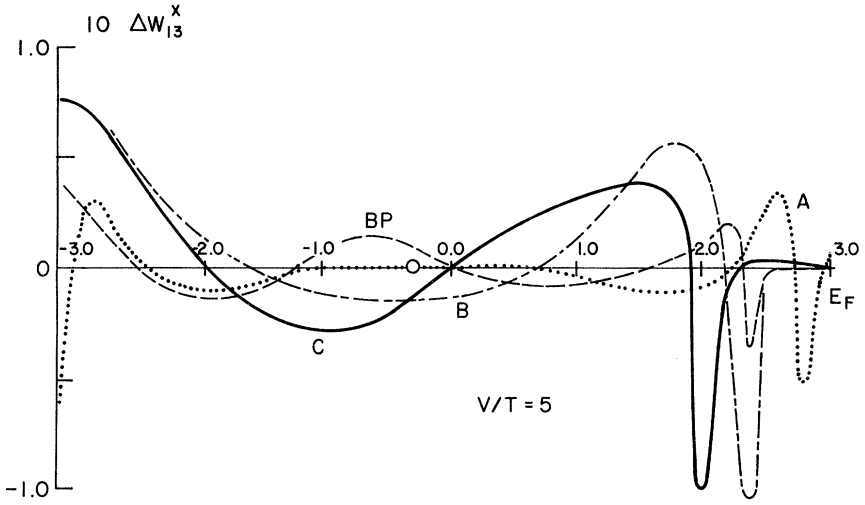

FIG. 8. Pair interaction for third-nearest neighbors with a potential in the split-off state regimes $E_a = -0.3$. For all but atop binding, splitting off below the band has been completed i.e., E_+, E_s, and E_- are all less than E_0. Near the upper band edge, precursor states appear.

by up to $\frac{1}{10} W_b$. In the ⟨11⟩ direction bridge and bridge perpendicular are identical, and their curve lies between centered and atop binding. The tracking relations begin to fail at the intermediate sites—$(ij) = (33)$ and (14), a distance between $2.5a_0$ and $3.5a_0$ from the origin—and collapse at the distant sites. At distant sites, most of the variation of ΔW^X_{ij} is concentrated in a sharp center peak for E_F near the bottom of the band for strong V and near E_a for weak V. On the other hand, as the potential increases, the tracking relations improve in the sense that the curves grow remarkably similar in amplitude and in the position of extrema and nodes. For the strongest potentials, in fact, all four binding types track to a degree: While the number of nodes might differ, the over-all general shapes have similar patterns. The difference in number of extrema in the band for different sites and binding types leads to a multiplicity of patterns as the Fermi level rises, with some sites attractive and others repulsive in a rather unpredictable fashion. Obviously, since there are fewer oscillations for the nearest sites, they are the most stable to sign change as the band fills. Only near the bottom of the band (and when there are no states split off below it) do all eight independent sites (i.e., all 36 sites, by symmetries) have the same sign:

$$\Delta W^X_{ij}(E_F \gtrsim -\tfrac{1}{2} W_b) < 0 \quad .$$

This property is a consequence of remarks (v), (vii), and (viii), and can be verified by rewriting the integrand of (3.3) in the form of (3.4). Taking the logarithm breaks the expression into three summands. The imaginary part of the log, the arctangent, can be expanded to first order in the imaginary part over the real part of each of the three arguments, since $\mathrm{Im}G \to 0^+$ at the lower edge and the denominator is finite and negative when there are no split-off states. A bit of algebra and

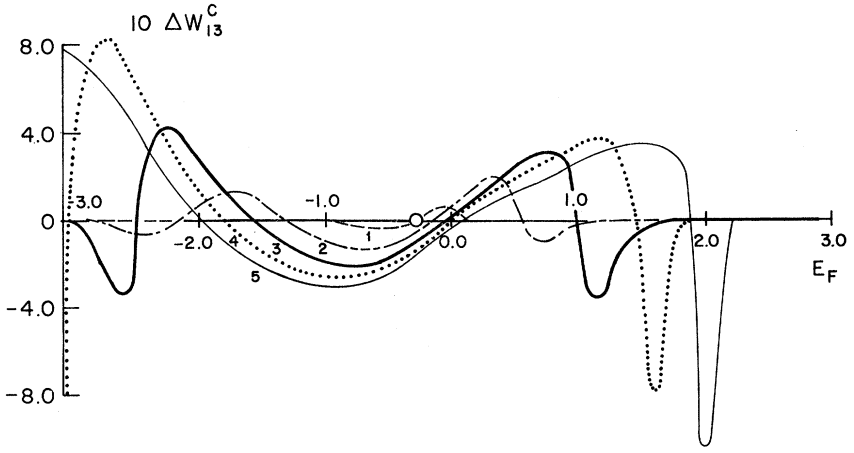

FIG. 9. Pair interaction for third-nearest neighbors, with bridge binding and $E_a = -0.3$, illustrating the effect of increasing the potential from $V/T = 1$–5 in integer steps. For stronger potentials, the curves in the interior of the band merely increase in amplitude with increasing potential, with little change in shape. At the lower band edge, one sees the evolution of a split-off state: for $V/T = 3$, there is a precursor; for $V/T = 5$, splitting off is completed.

the fact that $\mathrm{Re}G^X_{ij}(-\frac{1}{2}W_b)<0$ shows the integrand to be positive, and hence ΔW to be negative initially.

The large number of sites along the ⟨10⟩ direction for which ΔW_{pair} is calculated enables us to say something meaningful about the decrease in the interaction energy with distance in the local (nonasymptotic) regime for potentials sufficiently weak so that no split-off states occur. For $V/T \gtrsim 4$, numerical difficulties preclude any quantitative discussion of the distant sites; hence the subsequent paragraph is restriced to $V/T \lesssim 3$. We find an exponentiallike dropoff with roughly the form

$$|\Delta W_{ij}| \approx \gamma e^{-\beta(j-1)} = \gamma e^{-\beta R/a_0}\ , \qquad (3.5)$$

where γ is of order unity for $V/T=3$. The best value for β is about $\frac{5}{3}$ or 2, depending on how one measures the amplitude of ΔW_{ij}. If one characterizes the interaction by the largest absolute magnitude of $\Delta W^X_{ij}(E_F)$ for the Fermi energy at any place within the band (as one must for localized binding), then the lower value of β applies, giving a dropoff of about $\frac{1}{5}$ (though ranging from $\frac{1}{10}$ to $\frac{1}{3}$) in the pair interaction as the separation between the adatoms increases by one lattice constant.

This method is used in Fig. 10, which substantiates the claim of exponential falloff with increasing pair separation. A second method characterizes ΔW^X_{ij} by an envelope containing most extrema but excluding unusually large isolated peaks; this viewpoint gives a range of $\frac{1}{12}$ to $\frac{1}{4}$ for the falloff ratio per lattice constant. If we examine the actual falloff ratios as a function of separation, we find a nonmonotonic behavior that is distinctly not inverse powerlike in the range of pair distances considered. Our preliminary analysis suggests that the asymptotic form of the interaction energy goes as an inverse power, but as R^{-5} rather than as the familiar R^{-3} which occurs for bulk impurities. In any case, a virtual-level approximation, as enunciated by Grimley and Walker,[6] marked by inverse-power behavior even for small separations between adatoms, seems quite poor for the range of V considered here. The Green's functions are highly energy dependent, and of magnitude comparable to the energy parameter.

Again, we attempt to fit the dependence on potential to a relation of the form $\Delta W_{ij} \propto (V/T)^{\alpha}$, where α ranges from 4 in the perturbation limit down to 0 in the surface-molecule regime (1 in

TABLE II. Display of the pair-interaction energy suggesting the sensitivity of adatom arrays to changes in the Fermi level, the hopping potential, the adatom noninteracting level, and the binding type. One adatom sits at the origin (11) (denoted "0"); the pair energy for a second adatom at each of the nearby sites is indicated by the number at the site. The magnitude of the number given is 10 plus the common logarithm of the magnitude of the interaction. A plus (minus) sign means that the interaction is repulsive (attractive). Thus, $\Delta W=-2.7\times10^{-4}$ would be represented by -6.4 in the table. Each chart is labeled by the symmetric surface array predicted. Since ΔW_{ij}, $j\geq 4$, is unimportant for this determination, only $X=C$ is shown.

ΔW^X_{ij} $X=$		A			C						B			BP		
	31	32	33	31	32	33				31	32	33	31	32	33
$ij=$	21	22	23	21	22	23				21	22	23	21	22	23
	11	12	13	11	12	13	14	15	16	11	12	13	11	12	13
$E_F=1.2$	−7.7	−7.5	+7.5	−8.3	+7.1	−7.4				+8.4	+8.3	−6.1	−7.9	−7.4	−6.1
$E_a=-0.3$	+8.9	−8.1	−7.5	−9.0	−8.0	+7.1				−9.3	−8.4	+8.3	+8.2	−8.4	−7.4
$V/T=3$	0	+8.9	−7.7	0	−9.0	−8.3	−6.6	+6.1	+4.6	0	−9.3	+8.4	0	+8.2	−7.9
		$c(2\times2)$			(1×1)						(1×1)			$c(2\times2)$	
$E_F=1.2$	−7.8	−6.7	+7.4	−8.6	−6.2	−7.8				+8.7	+8.1	−7.6	+7.6	+7.0	−7.6
$\rightarrow E_a=-0.0$	+8.8	−8.4	−6.7	−9.4	−8.6	−6.2				−9.3	−8.3	+8.1	+9.0	−8.3	+7.0
$V/T=3$	0	+8.8	−7.8	0	−9.4	−8.6	+7.7	−5.8	+5.3	0	−9.3	+8.7	0	+9.0	+7.6
		$c(2\times2)$			(1×1)						(1×1)			$c(2\times2)$	
$E_F=1.2$	−7.7	+7.7	+6.9	+8.5	−7.5	+7.8				+8.5	−7.9	−7.8	−7.8	+6.9	−7.8
$E_a=-0.3$	+8.6	−8.6	+7.7	−9.3	−8.4	−7.5				−9.1	+7.5	−7.9	+9.1	+7.5	+6.9
$\rightarrow V/T=4$	0	+8.6	−7.7	0	−9.3	+8.5	+7.6	−6.1	+4.9	0	−9.1	+8.5	0	+9.1	−7.8
		$c(2\times2)$			(1×1)						(1×1)			(2×2)	
$\rightarrow E_F=0.9$	−7.5	+7.7	−7.0	+8.1	−7.9	+7.7				+8.4	−7.7	−7.7	+6.3	+7.8	−7.7
$E_a=-0.3$	+8.5	−8.5	+7.7	−9.3	−8.4	−7.9				−9.2	−7.1	−7.7	+9.0	−7.1	+7.8
$V/T=3$	0	+8.5	−7.5	0	−9.3	+8.1	+7.5	−6.3	+4.7	0	−9.2	+8.4	0	+9.0	+6.3
		$c(2\times2)$			(1×1)						(1×1)			$c(2\times2)$	
$\rightarrow E_F=1.5$	−6.7	−7.8	+4.4	−7.3	+5.8	−6.8				−8.4	−7.7	+7.0	+6.7	−7.0	+7.0
$E_a=-0.3$	+8.7	+8.3	−7.8	+6.2	−7.2	+5.8				−8.9	+6.2	−7.7	−8.7	+6.2	−7.0
$V/T=3$	0	+8.7	−6.7	0	+6.2	−7.3	−6.3	+5.5	+4.5	0	−8.9	−8.4	0	−8.7	+6.7
		$c(4\times2)$			$c(2\times2)$						(1×1)			(1×1)	

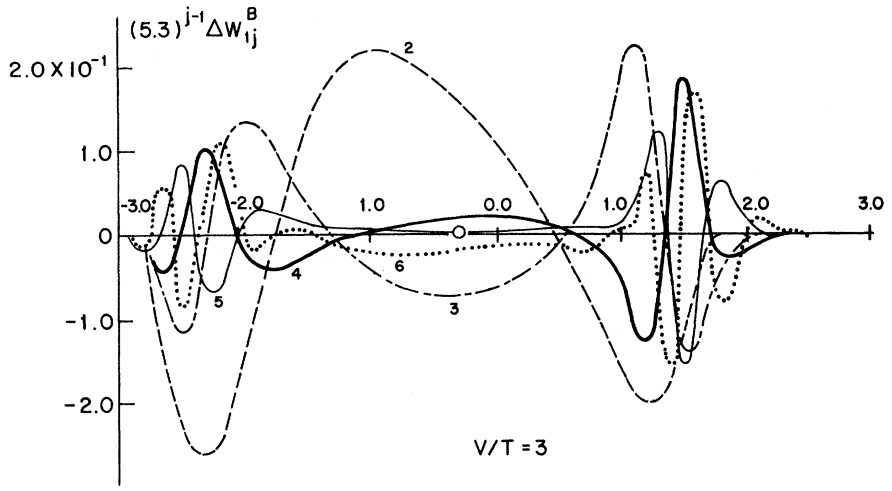

FIG. 10. Pair interaction, with bridge binding and $E_a = -0.3$, of adatoms separated by 1–5 lattice constants in the ⟨10⟩ direction. The curves are scaled by (5.3) raised to the separation minus one (in units of a_0), to show the exponential character of the decrease in interaction with increasing separation.

the special case of surface macromolecules mentioned at the end of Sec. II B 3). For peak-to-peak measurements with E_a near the band center, α averages 1.1 ± 0.7 in going from $V/T = 1$ to 2, and 3.4 ± 1.1 in going from 2 to 3. For envelope measurements between $V/T = 2$ and 3, α is $2.6 \pm \sim 1.0$ and 2.4 ± 0.5. We can alternatively consider the various γ. For $V/T = 1$, $\gamma \approx 0.2$; for $V/T = 2$, $\gamma = 0.4$ or 0.38 (method one or two). Hence, in going from 1 to 2, $\alpha \sim 1$, while going from 2 to 3. $\alpha \sim 2$. For stronger potentials, the features of the interaction curve in the interior of the band are relatively insensitive to variations of V; we can therefore focus attention on a particular interior extremum and compare its value for V/T ranging 3–5. We find that in general α is a fraction (between 0 and 1), and that α determined from $V/T = 3 \rightarrow 4$ is usually greater than α determined from $V/T = 4 \rightarrow 5$. (For the special cases of surface macromolecules, α is anomalously large, as expected from the discussion at the end of Sec. II B 3). We find it to lie between 1 and 2. Most importantly, we can definitely conclude that our parameters fall within the covalent area, as in the single-adatom case, and that the physical region is that in which we are approaching the surface-molecule limit.

Finally, we consider the dependence of ΔW^X_{ij} on the adatom level E_a. We recall that for the single-adatom problem, a shift of E_a by ΔE would roughly shift the interaction-energy extremum, and consequently the portion of the ΔW curve giving strongest binding, by ΔE along the E_F axis. For small shifts in E_a, and for both E_F and E_a not too close to a band edge, we can say that ΔW is locally well approximated by a function of only $E_F - E_a$. While a similar statement might be made for the case of two adatoms in the weakest potential, for stronger physical V we find this claim no longer so. In this range the interaction-energy curve (for E_F not near a band edge) is still basically just shifted along the E_F axis, but by an amount that is only a small fraction of ΔE. Figure 11 illustrates this behavior with $\Delta E = \frac{1}{6} W_b$. ΔW_{pair} cannot reasonably be fit by a function of $E_F - E_a$, even to lowest order. Moreover, it is not hard to show that in the unphysical limit of very strong potential (the asymptotic regime discussed at the end of Sec. II B 3), the dependence on E_a vanishes entirely. The weak dependence of ΔW^X_{ij} on E_a (compared with E_F) in the physical range (of V) is fortunate if one is trying to find the appropriate calculated curve for experimentally determined values of the input parameters E_a, E_F, W_b, and V (from heat of adsorption) since E_a is the most difficult of these four to determine: We recall from the discussion at the beginning of Sec. II B 2 that our E_a is in fact a rather phenomenological parameter which should be rescaled to give at least a Hartree–Fock account of the (nonmagnetic) Coulomb interaction U between an up- and a down-spin electron on the adatom. Clearly, in this approximation E_a is increased by U times the occupation number of the adatom for either spin direction; to lowest order this occupation number can be replaced by that for single-particle adsorption. [6]

C. Surface Arrays

Armed with a general understanding of the parametric dependence of the pair-interaction energy, we are ready to consider the surface arrays suggested by our results. In about half of the cases, the nearest-neighbor site is attractive ($\Delta W_{12} < 0$) and is the most attractive of any site. In these cases, the model suggests that a (1×1) adsorbate pattern form. However, in this case one can in general no longer legitimately neglect overlap effects—that is, the direct interaction between

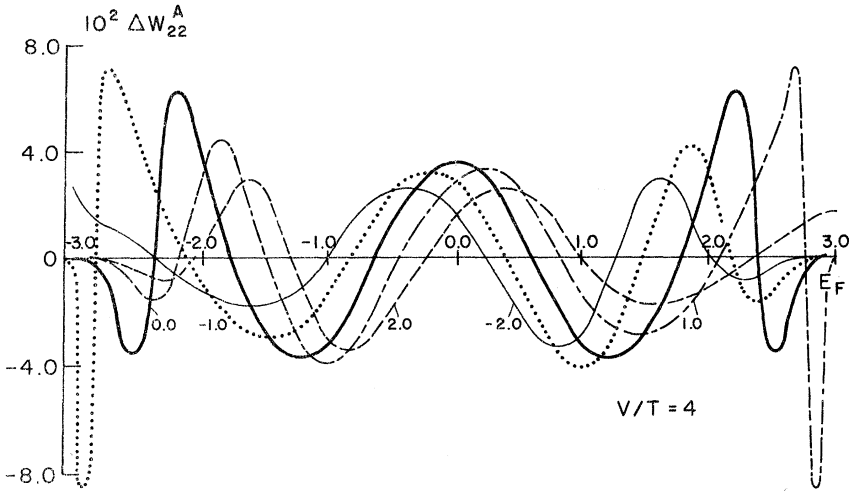

FIG. 11. Pair interaction for next-nearest neighbors, with on-site binding, for $E_a = -2.0$, -1.0, 0.0, 1.0, and 2.0. The curves verify the relative intensitivity of ΔW_{pair} to changes in E_a for physical potentials.

adatoms—so that the treatment here is unreliable for any details. Moreover, the model tends to overestimate the number of (1×1) arrays. Since all ΔW are negative near the lower band edge, and since ΔW_{12} has the fewest oscillations of all (ij) as a function of E_F, a disproportionate number of these (1×1) patterns fall near the edges (especially for weaker and intermediate potentials V), where not much dissociative chemisorption takes place. (Recall from Sec. III A that the binding energy is smallest near the band edges.) In general our model can suggest adlayers of the form $(k\times k)$ or $c(2k\times2l)$, k and l integers. Specifically, if the next-nearest-neighbor site, (22), is the most attractive, $c(2\times2)$ is favored; if (23) has ΔW most negative, $c(4\times2)$ has an energetic advantage; if (33) is most attractive, $c(4\times4)$ results; and if (13) is most negative, (2×2) should prevail [unless (22) is also attractive, in which case after some (2×2) growth the centered site will be filled, giving $c(2\times2)$]. As a rough check of general reasonableness, it is interesting to compare the frequency of occurrence of each array predicted by our model with that found by experiment, even though this procedure can do no more than establish that we are in the correct ballpark. From Somorjai and Szalkowski's[1] table summarizing surface arrays on substrates with fourfold symmetry, we extract the data for the binding of the simple (presumably single level) adparticles O, CO, H, and N, on the (100) surfaces of ten transition metals (so we hopefully get some average of E_F/W_b). Using no weighting factor, we count the number of occurrences of each of the four binding arrays our model predicts. There are seven occurrences each of (1×1), (2×2), and $c(2\times2)$, plus three cases of $c(4\times2)$.[17] (Also there were single instances of seven other surface lattices.) Neglecting (1×1) structures—for the overlap question mentioned above and because the table underestimates the frequency of (1×1) patterns in nature[1]—our calculation predicts remarkably similar ratios. In the band range $-1.8 \leq E_F \leq 1.8$ and for the gamut of parameters without or with split-off states, assuming uniform weighting of parameters, we find roughly the same number of (2×2) and $c(2\times2)$ (slightly more of the lattice), and about $\frac{1}{2}$–$\frac{3}{4}$ as much $c(4\times2)$ patterns.

As forecast by the preceding discussion of general properties, the viability of a particular pattern for a particular binding type is quite dependent on the parameters, particularly for weak potential. A change of E_a or especially E_F by $\frac{1}{20}W_b$ within the band interior will destroy a particular non-(1×1) array's energy advantage about a half to a third of the time—for stronger V, the latter factor being much more typical. Changing the potential from weak to intermediate has a more potent effect, altering structure in about $\frac{3}{4}$ of the instances. On the other hand, going from intermediate to strong potential, there is remarkably little change in structure. In going from $V/T = 4$–5, with all other parameters fixed, the pattern changes significantly for only about $\frac{1}{5}$ of the "samples." Finally, changing binding symmetry has a far more profound effect than varying the parameters listed above: It is extremely rare that for the same E_F, E_a, and V, more than two of the four types will exhibit the same pattern. This is to be expected from Figs. 6–8.

We do have one reliable test for the interaction energy of a $c(2\times2)$ pattern. To a fairly good approximation one can view this structure as a two-dimensional square-lattice gas with repulsive nearest-neighbor interaction and attractive next-nearest interaction (and neglect more distant interactions). Recalling that a lattice gas is equivalent to the Ising model, we can use the results of

Fan and Wu for the Ising model with second-neighbor interactions.[18] Since electrons have spin $\frac{1}{2}$, to transfer between the two models we make the substitutions

$$w_1 \equiv \Delta W_{12}(E_F) = -4J$$

and

$$w_2 \equiv -\Delta W_{22}(E_F) = 4J' \ ,$$

where J and J' are the Ising nearest and next-nearest exchange constants, and w_1 and w_2 are both positive. The $c(2\times 2)$ structure falls into the domain called antiferromagnetic, for which the approximate solution for T_c,

$$e^{\beta w_1/2} = \sqrt{2}\, e^{-\beta w_2/2} + e^{-\beta w_2} \quad (\beta = 1/kT_c) \ , \qquad (3.6)$$

applies. This equation for the ordered lattice critical temperature T_c is accurate to within a few percent for $w_1 \gtrsim w_2$. Most of our patterns fall into this range, with w_2 ranging from about w_1 to an order of magnitude smaller. For $w_1 = w_2$, (3.6) becomes a cubic equation with the solution $e^{-\beta w_2/2} = 0.68946\ldots$ (as compared with a Padé-approximant value of $0.6837\ldots$); for $w_1 \approx 7.83 w_2$, one can show by direct substitution that $e^{-\beta w_2/2} = 0.909$. Consequently, βw_1 ranges from 0.747 to 0.648. Experimentally, the critical temperature is on the order of $\frac{1}{20}$ eV,[19] so that $w_1 \sim 0.037$–0.032 eV. In our units of $\frac{1}{6} W_b$, $w_1 \sim 0.04$ for $W_b = 5$ eV and $w_1 \sim 0.02$ for $W_b = 10$ eV. These values are in reasonable agreement with calculated w_1 for $V/T \cong 3$ and E_a near the band center.

IV. CONCLUSION

Within the context of a tight-binding model, we have carried out a calculation of the indirect interaction energy ΔW between a pair of atoms adsorbed on the (100) surface of a simple cubic solid. To ΔW must be added the direct interaction between the adsorbate atoms. The model involves four parameters, the bandwidth W_b and the Fermi energy E_F of the bulk solid, the atomic energy E_a of the free-adatom orbital φ_a, and the hopping matrix element V which mixes φ_a and the orbitals φ_i on the surface atoms at the adsorption site. Our procedure is to fix W_b and E_F from data on the bulk solid. For an assumed value of E_a, V is fixed to obtain the observed chemisorption energy for a single atom at low coverage. ΔW is then determined uniquely as a function of the positions of the adsorbates relative to the substrate.

Three binding symmetries have been considered, namely, atop (over a single surface atom), bridge (equidistant from two nearest-neighbor surface atoms), and centered [in the center of the four atom square on the (100) surface]. We have considered ΔW only for pairs of atoms of the same bonding type so that ΔW is a function of the discrete surface unit cell indices of the two adsorbates i and j.

Our work is related to that of Grimley, who calculated ΔW in the asymptotic limit of large spacing between adsorbates for a surface characterized by a parameter which allowed for variable reactivity with the adsorbates. The essential distinction between Grimley's work and the present analysis is that our model includes crystal structure effects and calculations are carried out numerically so that ΔW can be calculated as a function of adsorbate separation, even for closely spaced adsorbates. These differences are of considerable importance since we find the interaction is quite sensitive to the binding type and the interaction is of significant strength only for interadatom spacing of a few substrate lattice spacings or less, the interaction falling off in scale roughly exponentially for the first several lattice spacings, whereas Grimley found a power law for large spacings. Furthermore, the virtual level approximation of Grimley is probably not valid for parameters appropriate to observed binding energies, since split-off states occur in this range of coupling, i.e., a tendency for surface complexes to be formed, which then couple to the indented solid. Nevertheless, the present model is sufficiently crude that the calculations are primarily of qualitative significance, i.e., it is not possible to this stage to draw comparisons with specific systems. We note that the interaction at small spacing varies from attractive to repulsive, generally on the scale of the lattice spacing, with the sign of ΔW for a particular spacing varying moderately with E_F, and significantly less so with E_a and V for potentials of physical interest.

It is gratifying that one finds for a reasonable range of parameters that many of the overlayer structures observed in low-energy-electron-diffraction (LEED) data appear to be the stable structures based on the calculated ΔW curves. In addition, the rough agreement between the melting temperature for the $c(2\times 2)$ lattice of H on (100) W and that calculated from ΔW fit to the observed chemisorption energy shows that the scale of ΔW is correct. Estimates indicate that explicit 3, 4... body forces are negligible compared to the pair interaction even at high coverage.

A distinctive feature of this work is the strong dependence of ΔW on the symmetry of the adsorption site (relative to the substrate). Unfortunately, our present analysis does not permit the hazarding of predictions of which adsorption-site symmetry exists in particular experimental systems. Several new approaches to analyzing experimental data should, however, provide information on this subject: Park[20] has commented on effects of the antiphase relationship between surface subdo-

mains—certain LEED beams are broadened while others remain unchanged. In some cases, it becomes possible to distinguish bonding at fourfold symmetry sites (atop or centered) from that at twofold symmetry sites (bridge or bridge perpendicular). Andersson and Pendry[21] are using intensity versus energy LEED spectra to investigate the structure of the surface unit cell, in particular to deduce the spacing between adatoms and their substrate neighbors. Webb and associates[22] are seeking similar information from the kinematic (single-scattering) intensity, which they extract from (multiple-scattering) LEED data by averaging at constant momentum transfer.

The present analysis should be generalized in a number of directions. A more realistic substrate having d orbitals and self-consistent potential effects are clearly of importance. Clearly, the direct interaction between adsorbates must be added to ΔW in calculating the properties of tightly packed overlayers.

ACKNOWLEDGMENTS

We would like to thank Professor Paul Soven and Professor Peder J. Estrup, as well as D. Kalkstein and R. H. Paulson, for many helpful discussions regarding the above problems.

---

*Work supported in part by the National Science Foundation and the Laboratory for Research on the Structure of Matter, University of Pennsylvania, of the Advanced Research Projects Agency.

[1]G. A. Somorjai and F. Z. Szalkowski, J. Chem. Phys. 54, 389 (1971), who reference most of the current experimental observations of patterns and offer a lucid discussion of nomenclature. This listing, however, suggests that the (1×1) pattern occurs roughly as often as $c(2\times2)$ or (2×2). In fact, (1×1) is the most frequently achieved pattern, by a substantial margin. It is however, far more difficult to detect from LEED patterns and also less interesting to deal with; Peder J. Estrup, private communication.

[2]J. Koutecký, Trans. Faraday Soc. 54, 1038 (1958).

[3]C. Kittel, *Quantum Theory of Solids* (Wiley, New York, 1963), p. 360, who references the pioneering RKKY papers.

[4]T. B. Grimley, Proc. Phys. Soc. (London) 90, 751 (1967).

[5]T. B. Grimley, Proc. Phys. Soc. (London) 92, 776 (1967).

[6]T. B. Grimley and S. M. Walker, Surface Science 14, 395 (1969).

[7]D. M. Newns, Phys. Rev. 178, 1123 (1969).

[8]P. W. Anderson, Phys. Rev. 124, 41 (1961).

[9]David Kalkstein and Paul Soven, Surface Science 26, 85 (1971).

[10]P. W. Tamm and L. D. Schmidt, J. Chem. Phys. 51, 5352 (1969).

[11]T. B. Grimley, Proc. Phys. Soc. 72, 103 (1958).

[12]S. Alexander and P. W. Anderson, Phys. Rev. 133, A1594 (1964); T. Moriya, Progr. Theoret. Phys. (Kyoto) 33, 157 (1965); S. H. Liu, Phys. Rev. 163, 472 (1967).

[13]B. Caroli, J. Phys. Chem. Solids, 28, 1427 (1967).

[14]D. E. Eastman, J. K. Cashion, and C. A. Switendick, Phys. Rev. Lett. 27, 35 (1971).

[15]D. J. Kim and Y. Nagaoka, Progr. Theoret. Phys. (Kyoto) 30, 743 (1963).

[16]R. P. Messmer and A. J. Bennett, Phys. Rev. B 6, 633 (1972).

[17]It is interesting to ask which of these cases have small enough work-function changes to indicate neutral rather than ionic chemisorption. Unfortunately, only half the references given by Somorjai and Szalkowski include information on $\Delta\varphi$. Using the criterion that ionic effects are important when $\Delta\varphi > (1/4)$ eV, we find that just less than half of those specifying $\Delta\varphi$ correspond to neutral adsorption, so our sample is hardly statistical. In this select group, we find a single case each of (1×1), (2×2), and $c(4\times2)$, and two examples of $c(2\times2)$, in reasonable agreement with predictions.

[18]Chungpeng Fan and F. Y. Wu, Phys. Rev. 179, 560 (1969).

[19]For example, Peder J. Estrup, in *The Structure and Chemistry of Solid Surfaces*, edited by Gabor A. Somorjai (Wiley, New York, 1969), Chap. 28.

[20]Robert L. Park, in Ref. 19, Chap. 28.

[21]S. Andersson and J. B. Pendry, J. Phys. C 5, L41 (1972).

[22]Max G. Lagally, Tran C. Ngoc, and M. B. Webb, Phys. Rev. Lett. 26, 1557 (1971); J. Vac. Sci. and Tech. 9, 645 (1972).